nature neuroscience

ARTICLES

https://doi.org/10.1038/s41593-018-0071-y

Insular cortex mediates approach and avoidance responses to social affective stimuli

Morgan M. Rogers-Carter, Juan A. Varela, Katherine B. Gribbons, Anne F. Pierce, Morgan T. McGoey, Maureen Ritchey and John P. Christianson*

Social animals detect the affective states of conspecifics and utilize this information to orchestrate social interactions. In a social affective preference text in which experimental adult male rats could interact with either naive or stressed conspecifics, the experimental rats either approached or avoided the stressed conspecific, depending upon the age of the conspecific. Specifically, experimental rats approached stressed juveniles but avoided stressed adults. Inhibition of insular cortex, which is implicated in social cognition, and blockade of insular oxytocin receptors disrupted the social affective behaviors. Oxytocin application increased intrinsic excitability and synaptic efficacy in acute insular cortex slices, and insular oxytocin administration recapitulated the behaviors observed toward stressed conspecifics. Network analysis of c-Fos immunoreactivity in 29 regions identified functional connectivity between insular cortex, prefrontal cortex, amygdala and the social decision-making network. These results implicate insular cortex as a key component in the circuit underlying age-dependent social responses to stressed conspecifics.

Social animals have an enormous repertoire of behavioral expressions that enable the transmission of affect to other members of the group[1]. Sensory and perceptive systems in the 'social decision-making network' (SDMN) allow one to appraise these social stimuli and integrate them with past experiences, as well as with situational and somatic factors, to shape specific social affective behavioral responses[2]. In addition to the SDMN, growing evidence implicates insular cortex in responding to social affective stimuli in humans. Specifically, emotion recognition and empathic deficits occur after insular cortex lesions[3–5], and empathic deficits in autism spectrum disorder (ASD) are related to insular cortex activity and connectivity[6–9].

The relationship between insular cortex and social affect in humans is likely a consequence of insular connectivity to sensory systems, which position it as locus of multisensory integration[10]. Notably, insular cortex is interconnected with the SDMN; this connectivity includes inputs from the hypothalamus[11] and ventral tegmental area[12], reciprocal connections with the amygdala[13], and outputs to periaqueductal gray[14], bed nucleus of the stria terminalis, nucleus accumbens[15] and medial prefrontal cortex[16]. The insular cortex also receives input from oxytocin (OT)-containing axons from the paraventricular nucleus[17], and OT-receptor (OTR) binding is enriched in the insular cortex[18]. OT modulates social behaviors across species[19], including empathic cognition in both humans[20] and rodents[21]. OT relieves social deficits observed in ASD and augments insular activity and connectivity[22,23], suggesting a mechanistic relationship between OT, insula and social cognition.

Translational rodent models that capture aspects of social affect include emotion contagion and social buffering[24]. However, some models require learning or direct exposure to a conspecific in pain, making it difficult to isolate social affective processes from other motivations[21,25]. We developed a rat social affective preference (SAP) test in which social affective behaviors were objectively quantified as a preference to approach or avoid interaction with a conspecific that had received a mild stressor. Because the experimental rat in the SAP test was not exposed to, nor witness to, the stressor itself, the unconditioned behavior of the experimental subject toward the conspecifics can be interpreted as a response to the affective state of the conspecific. We report a set of in vivo and in vitro studies that implicate insular cortex activity and modulation by OT as necessary and sufficient for modulating social affective behaviors in rat. Graph-theory-based network analyses[26] were performed to characterize, in rats, the relationship of the insular cortex to several regions of interest (ROIs) implicated in social decision-making.

Results

Age and stress exposure of conspecific determine social approach. In the SAP test, an experimentally naive adult male rat was presented with a pair of unfamiliar conspecific male stimuli (Fig. 1 and Supplementary Video 1). To manipulate social affect, one of the conspecifics was exposed to a mild stressor, consisting of two 5-s, 1-mA footshocks immediately before the test, while the other did not receive footshocks (naive). Because social approach behaviors are shaped, in part, by features of the target, including age[27], we hypothesized that the response of experimental rats to stressed conspecifics may depend on the conspecific's age. Twenty experimental adult male rats aged 60–80 d postnatal (PN 60–80) underwent SAP tests (Fig. 1a,b) in which the choice test involved exposure to a pair (one stressed, one naive) of unfamiliar male prepubertal juveniles or a pair of unfamiliar male adults[28]. The design was a 2×2 with conspecific age (PN 30 versus PN 50) as a between-subjects factor and conspecific affect (naive or stressed) as a within-subjects factor. We observed an increase in social interaction with the stressed juvenile (Fig. 1c; $P<0.0001$) but a decrease in interaction with the stressed adult ($P=0.020$). To summarize this interaction, we computed a percent preference score by dividing the time spent interacting with the stressed conspecific by the total time spent interacting during the test (Fig. 1d). Analysis of conspecific behavior revealed that stress caused juvenile conspecifics to engage in more self-grooming

Department of Psychology, Boston College, Chestnut Hill, MA, USA. These authors contributed equally: Morgan M. Rogers-Carter, Juan A. Varela. *e-mail: j.christianson@bc.edu

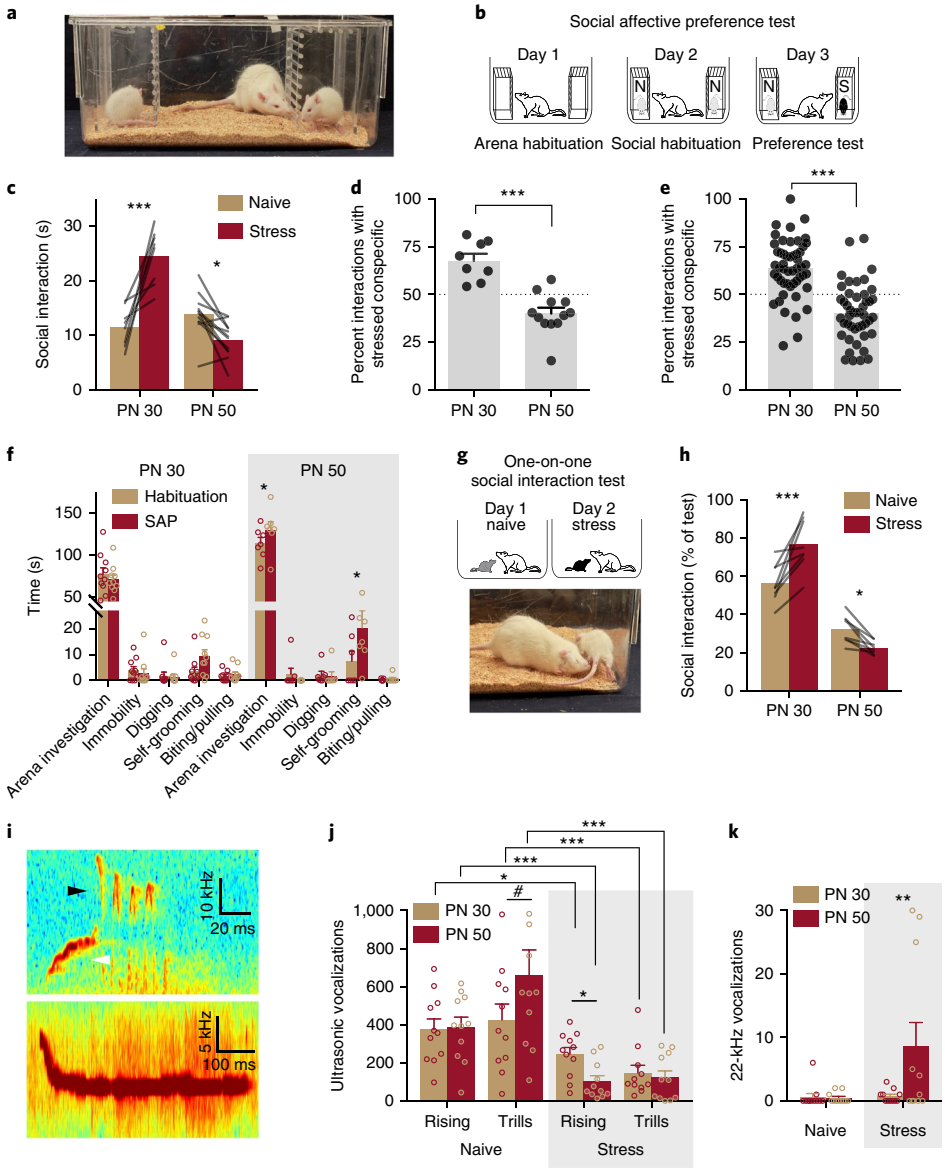

Fig. 1 | Social affective preference (SAP). a, The SAP arena, containing juvenile conspecifics on the left and right with an experimental adult in the center. **b**, Diagram of SAP test procedure with naive (N) or stressed (S) conspecifics. **c**, Mean (individual replicates shown as connecting lines) time spent in social interaction with the naive or stressed conspecific by age ($n = 8$ PN 30; $n = 12$ PN 50). A bidirectional effect of age was apparent in time spent interacting with the stressed conspecifics ($F_{AGE}(1, 18) = 27.93$, $P < 0.0001$; $F_{AFFECT}(1, 18) = 9.965$, $P = 0.006$; $F_{AGE \times AFFECT}(1, 18) = 46.05$, $P < 0.0001$). Experimental rats spent more time exploring the stressed PN 30 conspecific compared to the naive PN 30, but spent less time exploring the stressed PN 50 conspecific compared to the naive PN 50. **d**, Mean (± s.e.m. with individual replicates) data in **c** expressed as the percent of time spent interacting with the stressed conspecifics relative to the total time spent interacting. Experimental adults showed a marked preference (values greater than 50%) for interaction with stressed juvenile conspecifics and avoidance (values less than 50%) of stressed adults ($t_{18} = 5.783$, $P < 0.0001$, two-tailed). **e**, Mean (± s.e.m. with individual replicates, $n = 51$ PN 30, $n = 46$ PN 50) percent preference for interacting with the stressed conspecific pooled from all subjects in the experimental control groups included in the current report, including vehicle, sham and light OFF control groups of the later experiments. Percent preference scores for PN 30 and PN 50 interactions were significantly different ($t_{95} = 7.66$, $P < 0.0001$, two-tailed) from each other, and in both conditions the mean percent preference differed from 50% (PN 30: $t_{one\text{-}sample}(50) = 6.49$, $P < 0.0001$, two-tailed; PN 50: $t_{one\text{-}sample}(45) = 4.39$, $P < 0.0001$, two-tailed). **f**, Mean (± s.e.m. with individual replicates) time spent in nonsocial behaviors during habituation tests and SAP tests ($n = 10$ PN 30; $n = 7$ PN 50). More investigation of the arena and time spent self-grooming was observed in the PN 50 rats ($F_{AGE \times BEHAVIOR \times TEST}(4, 60) = 3.014$, $P = 0.025$). **g**, Diagram of one-on-one social interaction test and photo of typical adult-initiated interactions. **h**, Mean (individual replicates, $n = 8$ per age) time interacting with the naive or stressed conspecific in a one-on-one test, shown as percent of test time. Experimental adults spent significantly more time interacting with the stressed PN 30 conspecific but significantly less time with the stressed PN 50 conspecific compared to the respective naive conspecific targets ($F_{AGE}(1, 14) = 103.10$, $P < 0.0001$; $F_{AGE \times AFFECT}(1, 14) = 31.34$, $P < 0.0001$). **i**, Representative audio spectrograms depicting rising (top, white arrow), trills (top, black arrow) and 22-kHz USVs. Scale bars indicate *y*-axis ranges: 60–70 kHz (top) and 30–35 kHz (bottom). **j**,**k**, Mean (± s.e.m. with individual replicates, $n = 11$ per group) number of rising and trill USVs recorded during 5-min one-on-one social interactions. Fewer rising and trill calls were observed during interactions with stressed conspecifics, with fewer rising calls observed in stressed adults compared to stressed juveniles but more 22-kHz calls observed in stressed adults than stressed juveniles ($F_{STRESS}(1, 40) = 26.16$, $P < 0.0001$; $F_{CALL\ TYPE}(2, 80) = 60.86$, $P < 0.0001$; $F_{STRESS \times CALL\ TYPE}(2, 80) = 20.18$, $P < 0.0001$; $F_{CALL\ TYPE \times AGE}(2, 80) = 3.43$, $P = 0.37$). $^*P < 0.05$, $^{**}P < 0.01$, $^{***}P < 0.001$ (Sidak's tests).

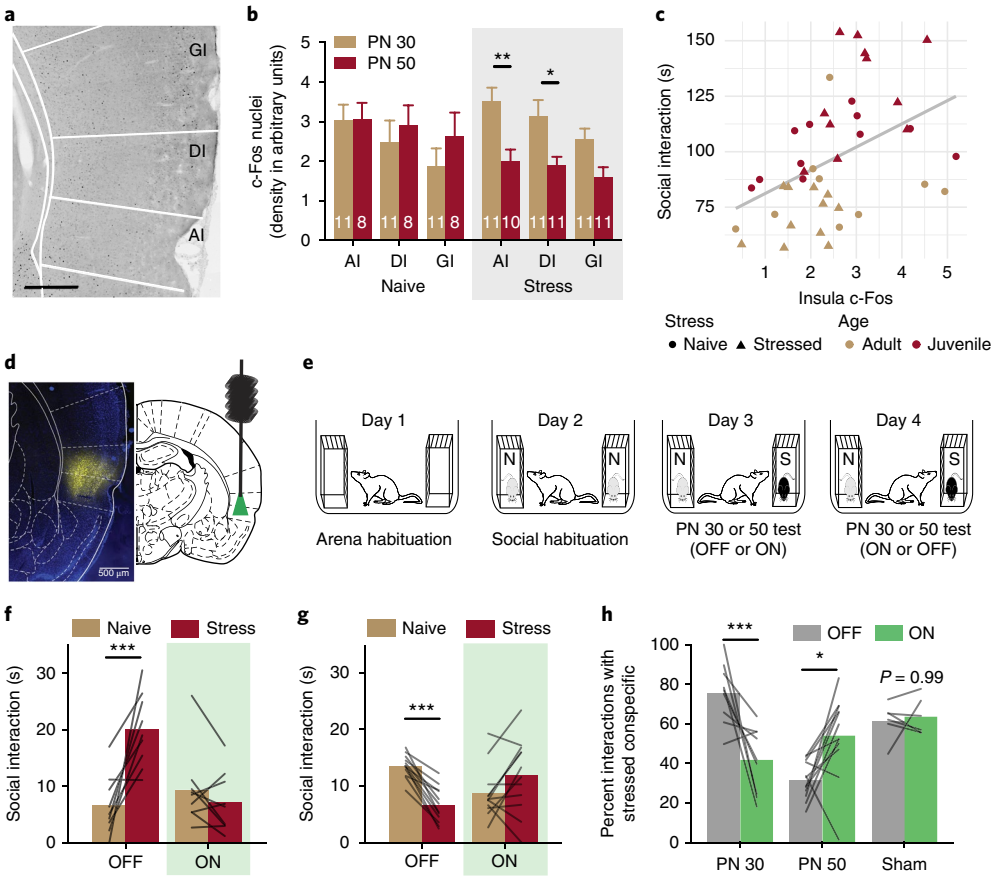

Fig. 2 | Optogenetic silencing of insular cortex during SAP tests. a, Representative digital photomicrograph containing insular cortex regions and c-Fos immunoreactive nuclei (black ovoid particles). AI, agranular; DI, dysgranular; GI, granular; scale bar, 500 µm. **b**, Mean (± s.e.m.; numbers indicate number of replicates) c-Fos immunoreactive nuclei by insular cortex subregion, quantified 90 min after social interaction with a naive PN 30, naive PN 50, stressed PN 30 or stressed PN 50 conspecific (5-min test). c-Fos was found in all regions, but there was an effect of stress for interactions with PN 50 rats, such that less c-Fos was evident after interaction with stressed PN 50 conspecific interactions than after interaction with naive PN 50 conspecifics, and there was less c-Fos in the AI and DI after interactions with stressed PN 50 rats than after interactions with stressed PN 30 rats ($F_{STRESS×AGE}(1, 36) = 6.21$, $P = 0.017$; $F_{SUBREGION}(2, 72) = 7.90$, $P = 0.001$). **c**, Mean c-Fos immunoreactivity (pooled across insula) predicted time spent in social interaction. Linear regression analysis (gray line) indicated a strong prediction of social interaction by c-Fos level and age and indicated modest interactions between stress, c-Fos and age ($F_{FOS}(1, 34) = 19.72$, $P < 0.0001$, $F_{AGE}(1, 34) = 36.93$, $P < 0.0001$; $F_{FOS×STRESS}(1, 34) = 3.97$, $P = 0.055$; $F_{STRESS×AGE}(1, 34) = 4.09$, $P = 0.051$). **d**, Native mCherry expression in the insular cortex (false-colored yellow) from a brain slice adjacent to one containing the cannula tract. (Scale bar, 500 µm). **e**, Diagram of SAP tests for optogenetic experiments. **f**,**g**, Mean time spent interacting with (**f**) PN 30 juvenile conspecifics ($n = 9$) or (**g**) PN 50 adult conspecifics ($n = 12$) on days 3 and 4 of the SAP test. In the light OFF condition, the experimental adult spent significantly more time interacting with the stressed PN 30 conspecific, but this pattern was abolished in the light ON condition ($F_{AGE×STRESS×LIGHT}(1, 19) = 41.31$, $P < 0.0001$). In the light OFF condition, the experimental adult spent significantly less time interacting with the stressed PN 50 conspecific, but this pattern was reversed in the light ON condition. **h**, Data from **f** and **g** converted to percent preference for interaction with stressed conspecifics. Here a clear age × light interaction is apparent, with optogenetic silencing of insular cortex eliminating the preference for interaction with the stressed juvenile and blocking the pattern of avoidance of stressed adult conspecifics ($F_{AGE×LIGHT}(1, 19) = 23.53$, $P = 0.0001$). No effect of optical stimulation was observed in sham-transduced rats. $^*P < 0.05$, $^{**}P < 0.01$, $^{***}P < 0.001$ (Sidak's tests). Brain Atlas illustrations were reproduced with permission as previously published in ref. [51], *The Brain Atlas in Stereotaxic Coordinates*, 4th Edition, Paxinos, G. & Watson, C. Pages 296, 303, 306–317 & 332. Copyright Elsevier (1998).

compared to the naive juvenile conspecific, but stress did not influence any other conspecific behaviors (Supplementary Fig. 1).

The SAP procedure was replicated several times in later optogenetic and pharmacology experiments, which provided a large sample size for evaluating the reliability and generality of these phenomena and for quantifying changes in experimental adult rat behavior from the habituation day to the SAP test day. Data from SAP tests conducted under either vehicle, light-OFF or sham treatments were pooled and converted to percent preference scores (Fig. 1e), and the scores were found to fit a normal distribution (D'Agostino and Pearson normality test, for PN 30: $K_2 = 2.52$, $P = 0.284$; for PN 50: $K_2 = 2.14$, $P = 0.343$). PN 30 and PN 50 preference scores normalized to the hypothetical value of 50% (equal time exploring both naive and stressed conspecifics, one sample *t* tests, two-tailed) revealed a preference for the stressed PN 30 ($P < 0.0001$) and a preference for the naive PN 50 ($P < 0.0001$). Approximately 82% (42 of 51) of rats tested with PN 30 conspecifics exhibited a preference for the stressed target, while only 21% (10 of 46) of rats tested with PN 50 conspecifics exhibited preference for the stressed target. The same pattern was also observed in SAP tests with female experimental adults (Supplementary Fig. 2). To evaluate whether exposure to the stressed conspecific in the SAP tests altered any other aspect of experimental adult behavior, we quantified behaviors of the experimental adult rats during habituation and SAP tests (Fig. 1f). While most behaviors measured were equal across tests, a significant age × behavior × test (habituation versus

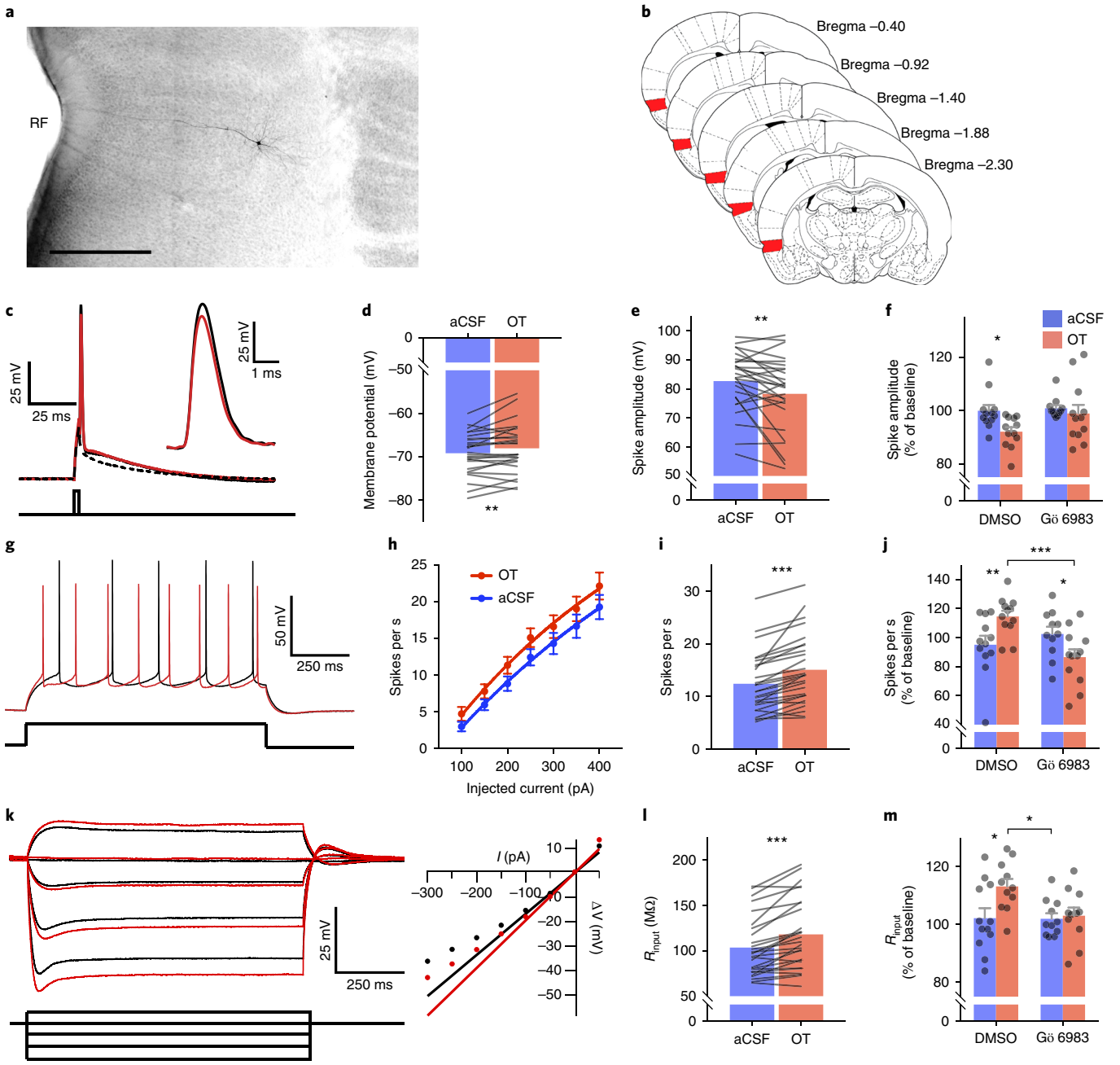

Fig. 3 | Intrinsic membrane properties in insular cortex pyramidal neurons are modulated by oxytocin and depend upon PKC. a, Digital photomicrograph of a typical biocytin filled neuron (RF, rhinal fissure; scale bar, 500 µm). **b**, Schematic diagram illustrating the ROI for whole-cell recordings (red shading). **c**, Typical action potential before (black dashed trace) and after bath application of 500 nM OT (red). Inset: detail of the action potential peak amplitude difference. Intrinsic properties were characterized from a sample of 27 neurons; the dependence of OT effects on PKC was determined by first characterizing the change in intrinsic properties from baseline followed by no treatment (artificial cerebrospinal fluid, aCSF) or OT (500 nM) in either the presence of DMSO buffer or DMSO and Gö 6983 (200 nM, aCSF+DMSO $n=12$; OT+DMSO; $n=12$, aCSF+Gö 6983; $n=11$; OT+Gö 6983, $n=12$). **d**, Mean action potential amplitude; OT significantly reduced amplitude. **e**, Mean resting membrane potential. OT significantly depolarized the membrane at rest. **f**, Mean action potential amplitude (± s.e.m. with individual replicates); OT significantly reduced spike amplitude but did not change in the presence of Gö 6983 ($F_{OT}(1, 21)=4.56$, $P=0.044$, aCSF vs. OT, $P=0.040$). **g**, Typical train of spikes evoked by 1-s 150-pA current injection before (black) and after (red) OT. **h**, Mean (± s.e.m.) spikes evoked by increasing current injections; OT increased the spike frequency ($F_{OT}(1, 279)=10.42$, $P=0.001$). **i**, Mean action potentials evoked by 250-pA current; significantly more spikes were evoked after OT. **j**, Mean (± s.e.m. and individual replicates) spike frequency upon 250-pA depolarization; OT increased spiking compared to aCSF, and Gö 6983 reduced spiking on its own ($F_{OT\times GÖ}(1, 43)=11.77$, $P=0.0013$, aCSF+OT vs. Gö 6983+OT, $P=0.0007$). **k**, Membrane potentials evoked by subthreshold and hyperpolarizing current injections (left) and typical rectification curve (right) before (black traces) and after (red traces) OT. **l**, Mean input resistance (R_{input}); OT significantly increased R_{input}. **m**, Mean (± s.e.m. and individual replicates) input resistance. OT increased input resistance ($F_{GÖ}(2, 20)=4.66$, $P=0.043$, OT+DMSO vs. OT+Gö 6983, $P=0.03$). Symbols and connecting lines indicate individual replicates. $^*P<0.05$, $^{**}P<0.01$, $^{***}P<0.001$ (Sidak's tests). Brain Atlas illustrations were reproduced with permission as previously published in ref. [55], *The Brain Atlas in Stereotaxic Coordinates*, 4th Edition, Paxinos, G. & Watson, C. Pages 296, 303, 306–317 & 332. Copyright Elsevier (1998).

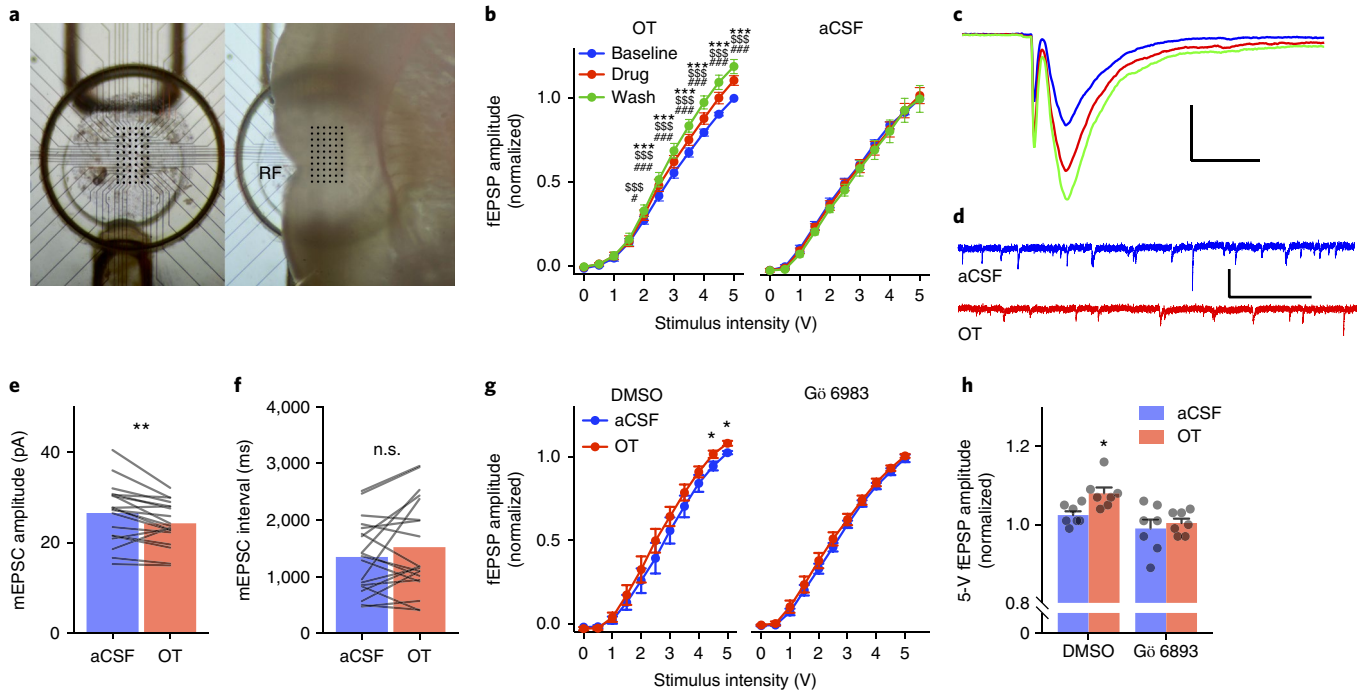

Fig. 4 | Oxytocin modulates excitatory synaptic transmission in the insular cortex. a, Top view of 60-channel perforated Multiple electrode array (left) for acute extracellular recordings of the insular cortex. Right: location of insular cortex slice during recording. **b**, Input-output curves for fEPSPs (mean ± s.e.m., OT $n=10$, aCSF $n=9$ slices) normalized to the peak amplitude observed in response to 5-V stimulation under baseline conditions. OT significantly increased EPSP amplitude beginning at 2 V with further enhancement during the washout ($F_{STIMULUS}(10, 90)=598.20$, $P<0.0001$; $F_{DRUG}(2, 18)=11.99$, $P<0.001$; $F_{STIMULUS\times DRUG}(20, 180)=11.34$, $P<0.0001$). Without application of OT, EPSPs remain stable across the duration of the experiment (aCSF: $F_{STIMULUS}(10, 80)=385.90$, $P<0.0001$). $^{\#\#\#}P<0.0001$ OT vs. baseline, $^{\$\$\$}P<0.0001$ washout (wash) vs. baseline, $^{***}P<0.0001$ wash vs. OT; Sidak's test). **c**, Typical fEPSPs evoked by biphasic extracellular stimulation at baseline (blue) during application of 500 nM OT (red) and after washout (green). Scale bar, 500 µV/ms. **d**, Representative voltage-clamp recordings of mEPSCs recorded before (aCSF; blue) and after OT (red). **e**, Mean mEPSC amplitude before and after OT ($n=19$ neurons); OT significantly reduced amplitude (paired $t_{18}=3.29$, $^{**}P=0.004$, two-tailed). **f**, Mean mEPSC interval ($n=19$ neurons); no effect of OT was apparent (paired $t_{18}=1.42$, $P=0.17$, two-tailed; n.s., not significant). **g**, Input-output curve for fEPSPs (mean ± s.e.m., $n=7$ slices per condition) normalized to the peak amplitude observed in response to 5-V stimulation under baseline conditions. OT (1 µM) increased fEPSP at 4.5 and 5 mV while no effect was observed in the presence of Gö 6983 ($F_{STIMULUS\times DRUG}(10, 240)=3.40$, $P<0.0003$. *OT vs. aCSF at 4.5 and 5 V, $P=0.0306$ and $P=0.0181$, respectively; Sidak's test). **h**, Mean (± s.e.m. and individual replicates) fEPSP amplitude from **g** at 5 V ($F_{OT}(1, 24)=5.076$, $P=0.034$ *OT+DMSO vs. aCSF+DMSO, $P=0.018$; vs. aCSF+Gö 6983, $P=0.002$; vs. OT+Gö 6983, $P<0.0004$; Fisher's Least significant difference test).

SAP) interaction ($P=0.025$) reflected increases in arena investigation ($P=0.05$) and self-grooming ($P=0.035$) during SAP tests with PN 50 conspecifics.

From the SAP test results, we predicted that in one-on-one interactions, an experimental adult should engage in more social interaction when exposed to a stressed juvenile than when exposed to a naive juvenile and should display the opposite pattern for adult targets. Experimental adult rats were given a series of two one-on-one social exploration tests (5-min duration, one test per day) with one unfamiliar naive PN 30 juvenile followed by one unfamiliar stressed juvenile as the social interaction targets (Fig. 1g); a separate set of experimental adults received the same series of tests with PN 50 adult conspecifics. A within-subjects design was used, with test order counterbalanced. As in the SAP test, experimental adults spent more time interacting with the stressed juvenile ($P=0.0002$) and less time with the stressed adult ($P=0.041$; Fig. 1; see Supplementary Fig. 2 for a serial variation of this test). There was no difference in conspecific-initiated social investigation at either age.

Conspecific stress alters ultrasonic vocalizations. Ultrasonic vocalizations (USVs) signal emotional states in rats[29]. To explore whether stress altered USVs during social interactions, a separate set of rats was given a 5-min one-on-one social interaction in a chamber equipped with an ultrasonic microphone. Social interaction and USVs were quantified during exposure to one of four conspecific stimuli: naive PN 30, naive PN 50, stressed PN 30 or stressed PN 50. Three types of vocalizations were present in our recordings: 22-kHz flat vocalizations, ~30- to 60-kHz rising calls and ~60- to 80-kHz trills (Fig. 1i and Supplementary Fig. 3). Rising and trill calls, which are emitted during and in anticipation of rewarding stimuli, were quite frequent during naive interactions but reduced during stressed interactions (Fig. 1j). The 22-kHz vocalizations are thought to convey negative affect, and these were observed primarily during interactions with stressed adults (Fig. 1k). More 22-kHz calls were evident in interactions with PN 50 stressed rats than with PN 50 naive ($P=0.0052$), PN 30 stressed ($P=0.0070$) or PN 30 naive ($P<0.0001$) rats; there were fewer rising calls in interactions with PN 30 or PN 50 stressed rats than with naive conspecifics ($P=0.0446$ and $P<0.0001$, respectively), more rising calls in interactions with stressed PN 30 rats than stressed PN 50 ($P=0.0304$), fewer trills in interactions with PN 30 and PN 50 stressed rats than with naive rats ($P<0.0234$ and $P<0.0001$, respectively) and a trend for more trills in the naive PN 50 compared to PN 30 ($P=0.055$). Although it is impossible to determine whether stress reduced USVs emitted by conspecifics, by the experimental rat toward the stressed conspecific or some combination of both, stressor exposure dramatically shifted the patterns of USVs consistent with a state of negative affect.

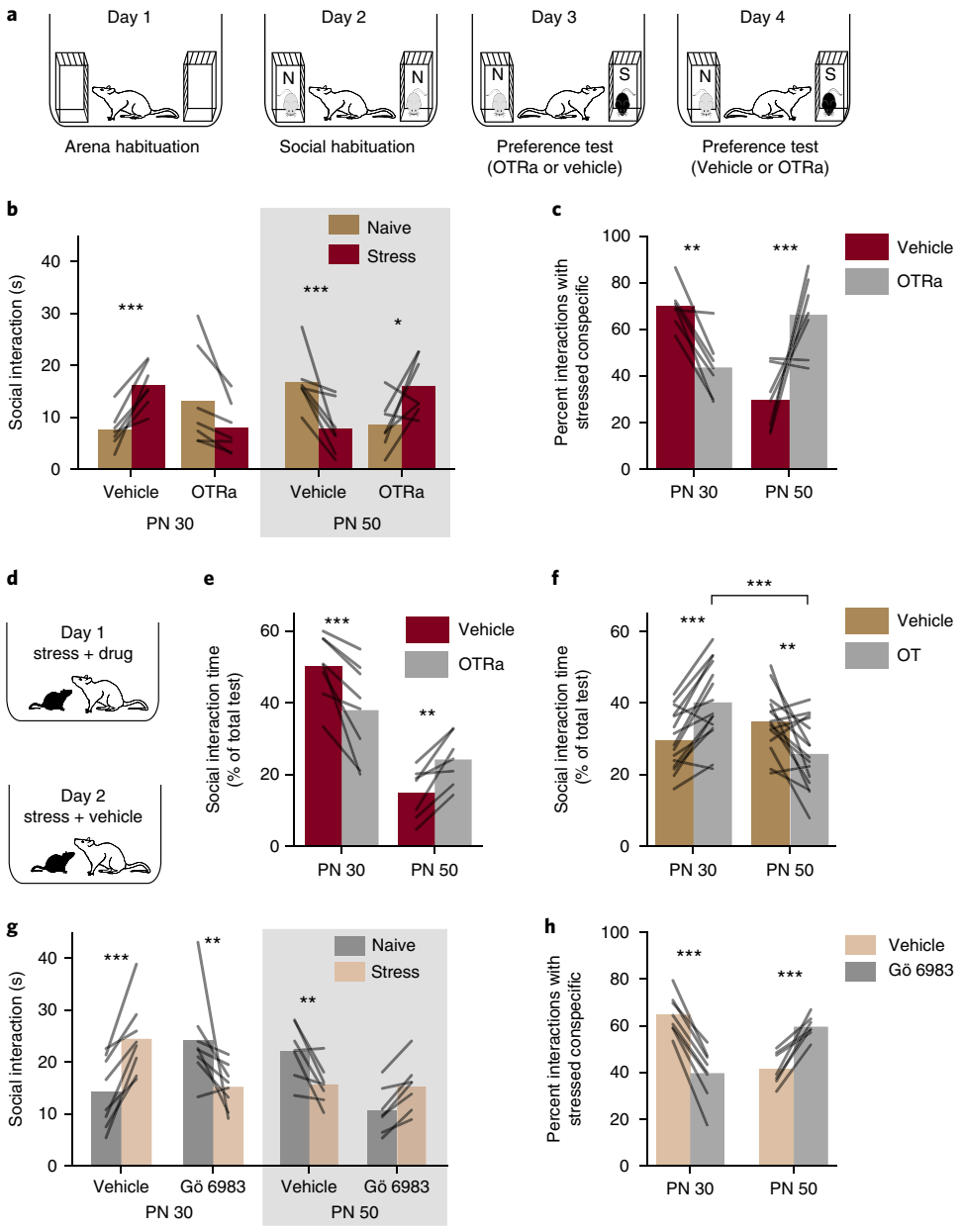

Fig. 5 | Social affective behaviors require insular cortex oxytocin. a, Diagram of experimental design. **b**, Mean (individual replicates) time spent exploring either PN 30 ($n=7$) or PN 50 ($n=7$) conspecifics after bilateral intra-insula infusion of OTRa (20 ng per side) in the SAP test. Vehicle-treated experimental adult rats spent more time interacting with the stressed than with the naive PN 30 juvenile conspecifics and less time with the stressed than with the naive PN 50 adult conspecifics. These effects were blocked and reversed, respectively, by infusion of OTRa ($F_{AGExDRUGxSTRESS}(1, 12)=31.843$, $P=0.0001$). **c**, Data in **b** expressed as percent preference for interaction with the stressed conspecific (mean with individual replicates). OTRa significantly reduced preference for the stressed PN 30 while increasing time spent with the stressed PN 50 conspecific ($F_{AGExDRUG}(1, 12)=26.38$, $P<0.0002$). **d**, Diagram of one-on-one social interaction tests with stressed conspecifics and pretreatment with either vehicle or OTRa. **e**, Mean (with individual replicates, normalized as percent of 3- to 5-min long test; time spent interacting with the stressed conspecific in a one-on-one test; PN 30: $n=8$, PN 50: $n=7$). OTRa significantly reduced time interacting with the stressed PN 30 conspecific but increased time interacting with the stressed PN 50 conspecific ($F_{AGE}(1, 13)=28.66$, $P<0.0001$; $F_{AGExDRUG}(1, 13)=32.56$, $P<0.0001$). **f**, Mean (with individual replicates) time spent interacting with a naive conspecific after intra-insular cortex OT (250 pg per side) or vehicle administration in a one-on-one social interaction (PN 30: $n=15$; PN 50: $n=15$). OT caused a significant increase in social interaction with naive PN 30 juveniles but a significant decrease in interaction with naive PN 50 adults ($F_{AGExDRUG}(1, 28)=30.08$, $P<0.0001$). **g**, Mean (individual replicates) time spent exploring either PN 30 ($n=8$) or PN 50 ($n=7$) conspecifics after intra-insula infusion of Gö 6983 (0.5 uL per side; 200 nM) or vehicle (10% DMSO in water) in the SAP test. Vehicle-treated experimental adult rats spent more time interacting with the stressed than with the naive PN 30 juvenile conspecifics and less time with the stressed than with the naive PN 50 adult conspecifics. These trends were blocked and reversed, respectively, by the PKC inhibitor ($F_{STRESSxAGExDRUG}(1, 13)=63.75$, $P<0.0001$). **h**, Data in **g** expressed as percent preference for interaction with the stressed conspecific (mean with individual replicates). Gö 6983 significantly reduced preference for the stressed PN 30 while increasing time spent with the stressed PN 50 conspecific ($F_{AGExDRUG}(1, 13)=141.10$, $P<0.0001$). *$P<0.05$, **$P<0.01$, ***$P<0.001$; Sidak's tests.

Table 1 | Effects of 500 nM OT on insular cortex pyramidal intrinsic membrane properties

Property	aCSF	500 nM OT	t_{26}	*P* value
Active	**Mean (s.e.m.)**	**Mean(s.e.m.)**		
Action potential threshold (mV)	-41.39 (0.83)	-41.89 (1.06)	0.893	0.380
Rheobase (pA)	1,507 (85.5)	1,429 (81.4)	3.217	****0.004**
Rise rate (mV/ms)	225.4 (13.04)	206.9 (13.42)	2.454	***0.021**
Spike amplitude (mV)	82.72 (1.95)	78.31 (2.46)	2.846	****0.009**
Spike width (ms)	1.13 (0.05)	1.20 (0.06)	2.487	***0.020**
Decay rate (mV/ms)	-84.52 (3.16)	-77.93 (3.54)	3.471	****0.002**
ADP (mV)	11.40 (0.84)	11.60 (0.91)	0.664	0.512
Passive				
Resting potential (mV)	-69.2 (0.9)	-68.1 (1.1)	2.705	***0.012**
Time constant (mV)	25.74 (0.51)	23.81 (0.68)	2.947	****0.007**
Input resistance (MΩ)	103.7 (6.23)	118.3 (7.46)	5.473	*****<0.001**
Rectification ratio	0.812 (0.015)	0.824 (0.015)	1.575	0.127
Sag (mV)	1.43 (0.22)	1.10 (0.15)	2.342	***0.027**
sAHP (mV × ms)	-320.3 (36.13)	-230.6 (31.49)	3.336	****0.003**

sAHP, slow after-hyperpolarization; $n = 27$ cells; $^*P < 0.05$, $^{**}P < 0.01$, $^{***}P < 0.001$.

Optogenetic silencing of insular cortex prevented social affective preference. To test whether exposure to stressed conspecifics influences insular cortex activity, experimental rats were killed for analysis 90 min after the one-on-one social interaction tests described for USV analysis, and brain sections containing the insular cortex were stained for c-Fos immunoreactivity (Fig. 2a). c-Fos immunoreactivity was higher in the insula of rats that had interacted with stressed PN 30 conspecifics than in rats that had interacted with stressed PN 50 conspecifics (Fig. 2b; $P = 0.009$), and insula c-Fos immunoreactivity was lower in rats after interaction with PN 50 stressed rats than in rats after interaction with PN 50 naive rats ($P = 0.038$; pooled across region). A linear regression analysis with Age and Stress conditions included as moderators indicated that insula c-Fos levels predict social interaction ($P < 0.0001$; Fig. 2c). Together with a pilot study in which pharmacological inhibition of the insula before SAP tests altered the pattern of behavior observed in experimental rats (Supplementary Fig. 4), these data suggest that the activity and, perhaps, output of the insular cortex are necessary for social affective behavior.

To inhibit insular cortex pyramidal neurons, experimental rats were transduced with halorhodopsin (AAV5-CamKIIα-eNpHR3.0-mCherry), which allowed reversible neuronal silencing (Fig. 2d; verification provided in Supplementary Fig. 5). Two weeks after virus infusion, rats underwent SAP tests in a two-age (juvenile or adult conspecific) × two-affect (naive or stress) × two-light (OFF or light ON) design (Fig. 2e). Green light (ON) or no light (OFF) was delivered to the insula continuously during the SAP test. As expected, the majority of rats in the OFF condition exhibited a preference for interacting with the stressed juvenile (9 of 12 experimental rats) and avoided the stressed adult (12 of 14 experimental rats), whereas experimental rats in the light ON condition avoided the stressed juvenile (Fig. 2f) or preferred interacting with the stressed adult (Fig. 2g; age × stress × light interaction, $P < 0.0001$). The five rats that did not exhibit the expected preference pattern in light OFF were analyzed separately (Supplementary Fig. 6). Pairwise comparisons in the juvenile + OFF condition identified an increase in interaction with the stressed juvenile compared to naive juvenile ($P = 0.0020$), whereas in the adult + OFF condition there was a significant decrease in interaction with the stressed adult conspecific compared to the naive adult conspecific ($P = 0.0121$). In the light ON condition, there were no significant differences in exploration times with naive versus stressed conspecifics in either age condition (PN 30, $P = 0.0722$; PN 50, $P = 0.0625$). Thus, silencing the insular cortex prevented the expression of social affective behaviors. Notably, optical treatment had no effect on rats with sham transfections when interacting with PN 30 conspecifics (Fig. 2h) and did not influence exploratory activity or general behavior in the SAP test (Supplementary Fig. 5).

Oxytocin alters the excitability of the insular cortex. The foregoing suggested that exposure to stressed conspecifics triggers a neurobiological response that alters insular cortex activity. Because OTRs are expressed in the insula and OT can modulate excitatory balance in cortical circuits[30], we hypothesized that OT could directly modulate insular cortex excitability. Active and passive intrinsic properties were characterized after bath application of OT (500 nM) in whole-cell pyramidal neuron recordings ($n = 27$ neurons; Fig. 3). A complete list of parameters measured is provided in Table 1. OT caused depolarization of the resting membrane potential, an increase in input resistance and a decrease in membrane time constant. These changes would permit the membrane to charge faster and reach the action potential threshold with less excitatory input. Indeed, OT also reduced the minimum current injection required to elicit an action potential (i.e., the rheobase) and reduced the slow after-hyperpolarization. Together, these changes suggest that in the presence of OT, insular cortex pyramidal cells might achieve greater spike frequency. Consistently, spike frequency increased in response to sustained depolarizing currents. Notably, after OT application, action potentials were smaller, with decreased amplitude, rise rate, decay rate and longer duration (half-width), which may indicate that the increase in firing frequency could come at a cost of reduced neurotransmitter release. OTR is thought to signal through the $G\alpha_{q11}$ signaling cascade to raise intracellular Ca^{2+} levels and activate protein kinase C (PKC)[31]. To test whether the changes in intrinsic and synaptic physiology caused by OT were mediated by PKC, we applied the pan-PKC antagonist Gö 6983 (200 nM) in whole-cell recordings with or without OT (500 nM). Gö 6983 prevented the decrease in spike amplitude (Fig. 3f), increase in firing frequency (Fig. 3j) and increase in R_{input} (Fig. 3m) that were evident in OT-treated neurons.

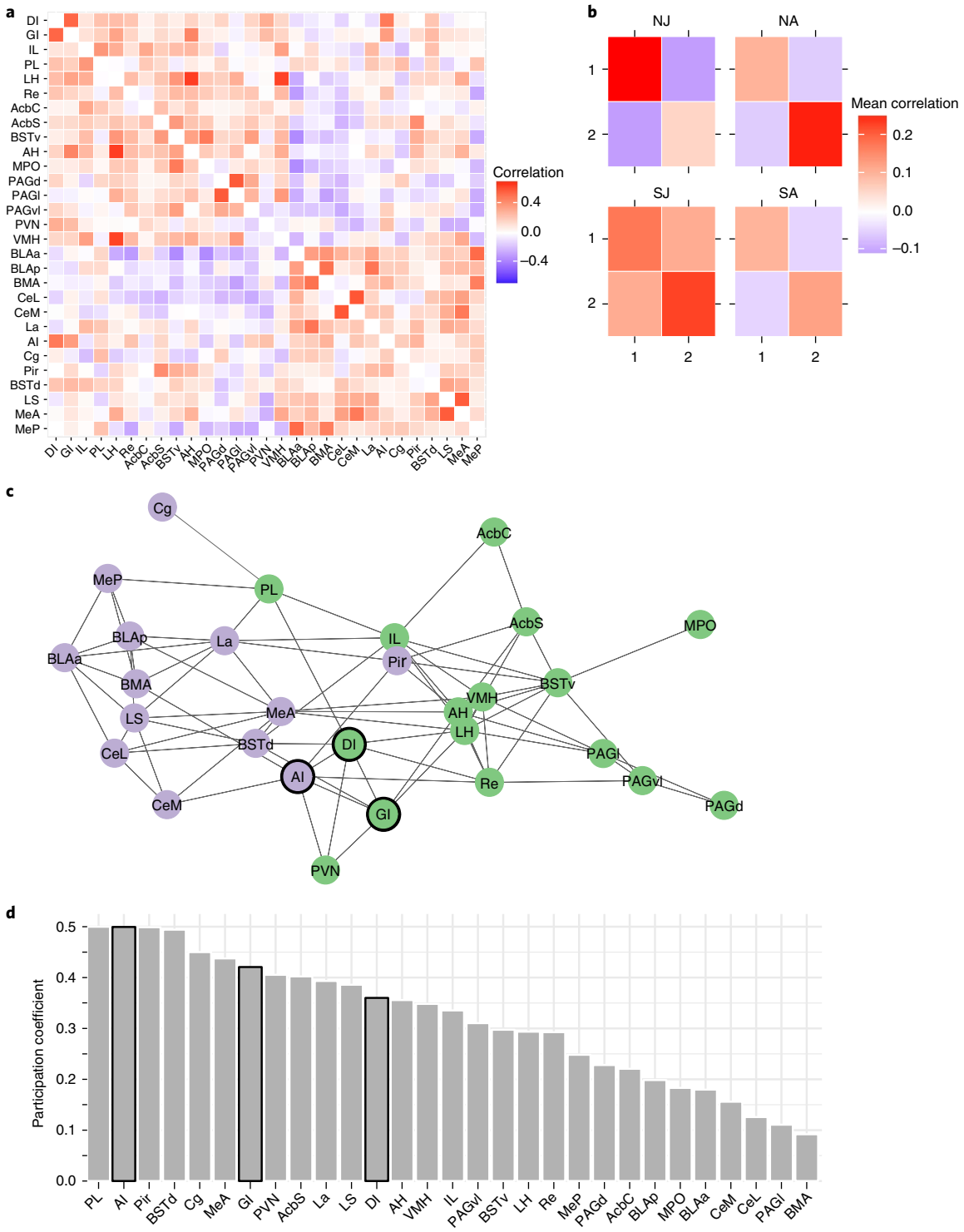

Fig. 6 | Insular cortex and the SDMN. c-Fos immunoreactivity was determined in 29 ROIs of the rats ($n = 44$) used in the USV quantification experiment (abbreviations provided in Supplementary Table 1 and representative images in Supplementary Fig. 7). **a**, Correlation matrix indicating functional correlations (Kendall's tau) among ROIs. **b**, Graph-theory-based community detection analyses identified two modules. Functional correlations within and between modules 1 and 2 were averaged across ROIs and shown for each group. **c**, Network visualization of the nodes in modules 1 (green) and 2 (purple). Here an arbitrary threshold of 0.2 was applied to facilitate network visualization, such that only edges exceeding the threshold are shown, but note that all network analyses were based on the unthresholded network. Insular cortex nodes are outlined in black. **d**, The degree to which each node is connected to multiple functional modules was estimated by computing the participation coefficient. Bars corresponding to insular cortex ROIs are outlined in black. Network analyses by treatment group provided in Supplementary Fig. 8. NJ, naive juvenile; NA, naive adult; SJ, stressed juvenile; SA, stressed adult.

To investigate the effect of OT on synaptic efficacy, input–output curves were conducted in acute insular cortex slices on a perforated 60-channel multiple electrode array (Fig. 4a–c). OT induced a leftward shift, with significantly larger field excitatory postsynaptic potential (fEPSP) amplitude compared to baseline at stimuli from 2 to 5 V with washout levels differing from OT beginning at

3 V ($P_s < 0.0001$). In the artificial cerebrospinal fluid control slices, synaptic responses were stable across all phases of the experiment. In the presence of Gö 6983 (200 nM), OT (1 μM) did not alter fEPSP input–output curves (Fig. 4g,h). Thus, OT augmented evoked excitatory synaptic transmission.

An increase in intrinsic excitability might also be reflected in a change in the miniature and/or spontaneous release of excitatory neurotransmitters in the slice. We made continuous whole-cell voltage-clamp recordings of deep-layer insular cortex pyramidal neurons ($n = 19$) before and after application of OT (500 nM) to quantify miniature excitatory postsynaptic currents (mEPSCs; Fig. 4d,f). OT reduced mEPSC amplitude ($P = 0.004$) but had no effect on mEPSC frequency. Taken together, the electrophysiology data suggests that OT rendered insular cortex pyramidal neurons more responsive to excitatory inputs via activation of PKC second-messenger cascades.

Insular cortex oxytocin receptors are necessary for both prosocial and asocial responses to stressed conspecifics. We next determined whether insular cortex OTRs contribute to the prosocial or asocial behaviors in the SAP test. Experimental rats ($n = 20$) were implanted with bilateral cannula guides to the insular cortex. Rats underwent the SAP procedure in a 2 × 2 × 2 experimental design with conspecific age (PN 30 vs. PN 50) as a between-subjects factor and with drug (vehicle or OTR antagonist (OTRa), 20 ng per side) and conspecific stress as within-subjects factors (Fig. 5a). The rats received microinjections 15 min before SAP tests on days 3 and 4, with drug order counterbalanced. The conspecific stimuli were always unfamiliar; no effect of test order was apparent. Two subjects in the PN 50 condition with misplaced cannula were excluded (Supplementary Fig. 6). In the vehicle condition, 7 of 10 experimental rats exhibited a preference for stressed over naive juveniles and 7 of the 8 experimental rats exhibited a preference for naive over stressed adults (Fig. 5b,c). Rats that did not exhibit preference in the vehicle condition were analyzed separately (Supplementary Fig. 6). There was a significant age × drug × affect interaction ($P < 0.0001$), with greater time spent investigating the stressed PN 30 conspecific (versus the naive PN30) and less time investigating the stressed PN 50 conspecific (versus the naive PN50) in the vehicle conditions ($P_s = 0.001$), but more time interacting with the naive PN 30 conspecific ($P = 0.06$) and less time with the naive PN 50 conspecific ($P = 0.014$) in the OTRa condition. Percent preference scores revealed an age × drug interaction ($P < 0.0001$), with opposing effects of OTRa in experimental rats' behavior toward PN 30 ($P = 0.011$) and PN 50 ($P = 0.002$) groups. Thus, blockade of insular cortex OTRs prevented the age-dependent approach and avoidance behavior in response to stressed conspecifics in the SAP test.

A separate set of rats ($n = 16$) was prepared with bilateral insular cannula as above and underwent one-on-one interactions with either a stressed PN 30 juvenile or a stressed PN 50 adult conspecific (between-subjects) 15 min after vehicle or OTRa injections (within-subjects) in a 2 × 2 design; drug order was counterbalanced by day as above (Fig. 5d). One experimental rat interacting with adult conspecifics had a misplaced cannula and was excluded. ANOVA revealed a main effect of age and age × drug interaction ($P_s < 0.0001$). The main effect of age indicates more interaction time with the stressed juveniles than the stressed adults. OTRa microinjection reduced the time spent interacting with the stressed PN 30 conspecifics ($P = 0.0008$) and increased the time interacting with stressed PN 50 conspecifics ($P = 0.009$) in the one-on-one tests (Fig. 5e).

Insular cortex oxytocin administration recapitulates social affective behaviors toward naive conspecifics. We next determined whether intra-insular OT administration was sufficient to increase or decrease experimental rat interaction with nonstressed PN 30 or PN 50 conspecifics, respectively. Bilateral insular cannula implants were made in 32 rats and after recovery each received two one-on-one social interaction tests (3-min duration) with unfamiliar naive PN 30 or PN 50 conspecifics. A within-subjects design was used, such that each rat received vehicle injections before one test and OT (250 pg per side; equivalent to 500 nM) before the other. Injections were made 15 min before testing and drug treatment order was counterbalanced. One rat from each age group did not receive injections and was removed from analysis. OT increased time spent interacting with the naive PN 30 conspecific ($P < 0.0005$) and decreased time with the naive PN 50 conspecific ($P = 0.002$; Fig. 5f).

Social responses to stressed conspecifics require insular cortex PKC. The foregoing suggested the possibility that behavioral responses to stressed conspecifics depend on modulation of intrinsic excitably in the insular cortex by OT, and so we predicted that interference with insular cortex PKC would mimic the effect of OTRa. Rats received bilateral insular cortex cannula implants and underwent SAP tests with pretreatment with either vehicle or Gö 6983. Eight of 10 rats exhibited preference for the stressed PN 30 conspecific after vehicle injection, and 7 of 11 rats avoided the stressed PN 50 conspecific (Fig. 5g). In these rats, Gö 6983 reversed the pattern observed under vehicle (age × stress × drug interaction; $P < 0.0001$). In tests with PN 30 conspecifics, experimental rats spent more time interacting with stressed than naive conspecifics after vehicle injection ($P < 0.0001$) and less time interacting with the stressed than naive conspecific after Gö 6983 injection ($P = 0.0090$). In tests with PN 50 conspecifics, the experimental rats spent less time interacting with the stressed conspecific in the vehicle condition ($P = 0.0057$) but equal time interacting with the stressed conspecific after Gö 6983 injection ($P = 0.1614$). To summarize the behavioral studies, experimental adult rats preferred to interact with stressed juveniles but avoided interaction with stressed adult conspecifics. In the insular cortex, optogenetic silencing, blockade of the OTR and inhibition of PKC each interfered with experimental rats' responses to stressed conspecifics, and OT administration was sufficient to reproduce the phenomena with naive conspecifics.

Insular cortex and the social decision-making network. The insular cortex is anatomically connected to the SDMN, prefrontal cortex and amygdala. We assessed insular functional connectivity using c-Fos analysis in 29 ROIs spanning the insular cortex, prefrontal cortex, extended amygdala and the SDMN (Supplementary Table 1 and Supplementary Fig. 7) in the 44 rats that were used for USV analysis. A data-driven community detection analysis revealed a network with two modules (Fig. 6a), in which ROIs were more highly correlated within each module than between modules (maximized modularity quotient = 0.59). The degree to which ROI Fos levels were correlated within and between modules varied across the groups, with generally stronger correlations in the stressed juvenile condition (Fig. 6b). The two modules contain ROIs that may be categorized generally as 'social' and 'emotional' areas, respectively (Fig. 6c). We evaluated the participation coefficient for each node (Fig. 6d and Supplementary Fig. 8); this is a measure of the degree to which nodes correlate with multiple modules and has been argued to be an appropriate measure of 'hubness' for correlation-based networks[32]. Agranular insular cortex was among the nodes with the highest participation coefficients along with prelimbic prefrontal cortex, piriform cortex and dorsal bed nucleus, regions that are associated with emotion contagion[33], social learning[34] and as a hub in the SDMN[2], respectively. Thus, data-driven network analyses revealed functional integration among regions in the social brain and suggest that the insula is positioned to interact with previously identified nodes important for social and affective behaviors.

Discussion

To better understand the neural basis of social affective behavior, we developed an SAP test in which the choice to approach or avoid a stressed conspecific could be quantified. In the SAP test, behaviors depended upon both the age and emotional state of the conspecific, which may reflect a species-specific adaptation in which social stress signals are danger cues when generated by an adult, but prosocial cues when generated by juveniles. In vivo pharmacological experiments, in vitro studies and network analyses suggest that exposure to a stressed conspecific evokes OT release within the insular cortex which, via modulation of insular cortex output neuron excitability, orchestrates species-specific, age-dependent approach or avoidance behaviors via modulation of the SDMN. These findings provide new insight into the neural basis of elementary social affective processes and, consistent with human neuroimaging work, warrant consideration of the insular cortex as an important component of the social brain.

A central ideal in social neuroscience is that social behaviors involve the integration of multisensory cues with situational and somatic factors[35]. In rodents, social communication of emotion occurs via chemosignals[36], vocalizations[29] and overt behaviors[37]. Footshocked rats emit social odors that can either attract conspecifics in social buffering or serve as social alarm signals[38]. Although we did not investigate chemosignals, these likely contribute to the behavior of the experimental rats in the SAP test. Regarding vocalizations, 22-kHz USVs are emitted as alarm signals, and frequency-modulating USVs are thought to convey positive affect[39]. Accordingly, 22-kHz vocalizations were nearly undetectable during naive–naive interactions, but increased dramatically when one of the conspecifics was a stressed adult. Frequency-modulating (rising and trill) calls preceded bouts of social interaction (Supplementary Fig. 3) and were abundant in naive–naive interactions but dropped considerably when one of the conspecifics had received footshocks, a pattern consistent with a negative affective state in the stressed conspecifics. Regarding overt behaviors, stress increased the amount of time juvenile conspecifics engaged in self-grooming. Thus, the experimental rat may draw from vocalizations, visible cues and chemical signals to compute the age and emotional state of the conspecific. Suitably, the piriform cortex and medial amygdala, key olfactory processing areas modulated by OT during social interactions[40], were found among the highest participation coefficients in the network analysis (Fig. 6d and Supplementary Fig. 8). Additional studies are needed to establish which stimuli emitted by stressed conspecifics determine social affective behaviors and how this information converges on the insular cortex.

The decision to avoid a stressed adult may be adaptive, as the stressed conspecific may be perceived as a social danger cue. On the other hand, it is difficult to pinpoint the motivation to approach the stressed juvenile. In human social behavior, features of the target stimulus, including age, are critical determinants of whether or not someone will approach, help or avoid another in distress[27], and there are examples of prosocial responses to stressed conspecifics in both voles[21] and mice[41]. These prosocial examples appear to have boundary conditions. First, prosocial effects are evident in pair-bonded voles and familiar female mice, but not between strangers or in male mice; this may also generalize to rats[42] (but see ref. [25]). An effect of the conspecific's age has not previously been investigated, and our results suggest that prosocial behaviors may occur toward unfamiliar conspecifics if they are juveniles, regardless of sex (Supplementary Fig. 2). Regardless of the motivation underlying the behavior of experimental rats in response to stressed conspecifics, the phenomenon reported here is direct evidence of what de Waal argued is the most elementary component of empathy: "that one party is affected by another's emotional or arousal state" (p. 282)[43]. The SAP test may provide a useful addition to the preclinical toolkit for investigating psychiatric diseases in which social behavior is impaired, such as autism and schizophrenia.

Insular cortex is positioned to integrate social affective stimuli as a nexus between multimodal sensory inputs and emotional, executive and social circuits in the limbic system[10]. Analysis of c-Fos immunoreactivity across ROIs representing these systems revealed several features of the network underlying social affective behavior. Highly correlated patterns of activity emerged in two modules (Fig. 6), which were composed primarily of structures found in the SDMN or the structures associated with emotion, such as the nuclei of the extended amygdala and prefrontal cortex. Insular cortex subfields were found in both of these modules, with a high degree of participation in both networks, suggesting, together with the established anatomical connectivity, that it may integrate social and emotional processes. These features may be key to understanding why inhibition of the insular cortex not just interfered with social affective preferences, but in fact reversed them (Supplementary Fig. 9). We hypothesize that exposure to stressed conspecifics elicits parallel activity within these modules, which compete for control to either approach or avoid. OT altered several properties of insular neurons that are consistent with such a modulatory role, namely a reduction in action potential amplitude, increase in R_{input}, increase in input–output relationships, reduction in slow after-hyperpolarization and potentiation of evoked insular fEPSPs. Indeed, OT can increase spike output in vivo[44], and our data suggest an intrinsic mechanism that may underlie shifts in synaptic efficacy and excitatory–inhibitory balance found in cortical regions where OT is critical for myriad social behaviors[30,34]. Thus, in concert with sensory cues that identify the age of the conspecific, OT may bias the output of insula efferents to the ventral striatum or prefrontal cortex to promote interaction with stressed juveniles or efferents to the basolateral amygdala to promote avoidance in response to stressed adults, as these are thought to be the proximal mediators of the rewarding, empathic and emotional aspects of social behavior, respectively[45].

Like social behavior itself, the effects of OT administration on social decision-making are sensitive to situational and interpersonal factors, with OT sometimes producing prosocial effects and at other times antisocial effects[46]; both were observed after insular OT administration. Abnormalities in emotion recognition are central to several psychiatric conditions, including ASD[47,48], in which OTR polymorphisms[49,50] and insular cortex hypofunction[8,9] are correlates of symptom severity. Our results suggest that disruption of insula function may be key to pathophysiology in behaviors that depend upon social decisions regarding the emotions of others. The SAP test and the network model of insular input to the SDMN presented here provide a platform for further research into the neuroanatomical and physiological systems that integrate social information with decision-making and behavior.

Methods

Methods, including statements of data availability and any associated accession codes and references, are available at https://doi.org/10.1038/s41593-018-0071-y.

Received: 18 January 2017; Accepted: 30 November 2017;
Published online: 29 January 2018

References

1. Darwin, C. *The Expression of the Emotions in Man and Animals*. (St. Martin's Press, London, New York, 1976). Julian Friedmann.
2. O'Connell, L. A. & Hofmann, H. A. The vertebrate mesolimbic reward system and social behavior network: a comparative synthesis. *J. Comp. Neurol.* **519**, 3599–3639 (2011).
3. Gu, X. et al. Anterior insular cortex is necessary for empathetic pain perception. *Brain* **135**, 2726–2735 (2012).
4. Ibañez, A., Gleichgerrcht, E. & Manes, F. Clinical effects of insular damage in humans. *Brain Struct. Funct.* **214**, 397–410 (2010).

5. Leigh, R. et al. Acute lesions that impair affective empathy. *Brain* **136**, 2539–2549 (2013).
6. Blanken, L. M. et al. Cortical morphology in 6- to 10-year old children with autistic traits: a population-based neuroimaging study. *Am. J. Psychiatry* **172**, 479–486 (2015).
7. Di Martino, A. et al. Relationship between cingulo-insular functional connectivity and autistic traits in neurotypical adults. *Am. J. Psychiatry* **166**, 891–899 (2009).
8. Morita, T. et al. Emotional responses associated with self-face processing in individuals with autism spectrum disorders: an fMRI study. *Soc. Neurosci.* **7**, 223–239 (2012).
9. Odriozola, P. et al. Insula response and connectivity during social and non-social attention in children with autism. *Soc. Cogn. Affect. Neurosci.* **11**, 433–444 (2016).
10. Gogolla, N. The insular cortex. *Curr. Biol.* **27**, R580–R586 (2017).
11. Allen, G. V. & Cechetto, D. F. Functional and anatomical organization of cardiovascular pressor and depressor sites in the lateral hypothalamic area. II. Ascending projections. *J. Comp. Neurol.* **330**, 421–438 (1993).
12. Ohara, P. T. et al. Dopaminergic input to GABAergic neurons in the rostral agranular insular cortex of the rat. *J. Neurocytol.* **32**, 131–141 (2003).
13. Shi, C. J. & Cassell, M. D. Cortical, thalamic, and amygdaloid connections of the anterior and posterior insular cortices. *J. Comp. Neurol.* **399**, 440–468 (1998).
14. Sato, F. et al. Projections from the insular cortex to pain-receptive trigeminal caudal subnucleus (medullary dorsal horn) and other lower brainstem areas in rats. *Neuroscience* **233**, 9–27 (2013).
15. Allen, G. V., Saper, C. B., Hurley, K. M. & Cechetto, D. F. Organization of visceral and limbic connections in the insular cortex of the rat. *J. Comp. Neurol.* **311**, 1–16 (1991).
16. Yasui, Y., Breder, C. D., Saper, C. B. & Cechetto, D. F. Autonomic responses and efferent pathways from the insular cortex in the rat. *J. Comp. Neurol.* **303**, 355–374 (1991).
17. Knobloch, H. S. et al. Evoked axonal oxytocin release in the central amygdala attenuates fear response. *Neuron* **73**, 553–566 (2012).
18. Dumais, K. M., Bredewold, R., Mayer, T. E. & Veenema, A. H. Sex differences in oxytocin receptor binding in forebrain regions: correlations with social interest in brain region- and sex- specific ways. *Horm. Behav.* **64**, 693–701 (2013).
19. Donaldson, Z. R. & Young, L. J. Oxytocin, vasopressin, and the neurogenetics of sociality. *Science* **322**, 900–904 (2008).
20. Shamay-Tsoory, S. G. & Abu-Akel, A. The social salience hypothesis of oxytocin. *Biol. Psychiatry* **79**, 194–202 (2016).
21. Burkett, J. P. et al. Oxytocin-dependent consolation behavior in rodents. *Science* **351**, 375–378 (2016).
22. Aoki, Y. et al. Oxytocin improves behavioural and neural deficits in inferring others' social emotions in autism. *Brain* **137**, 3073–3086 (2014).
23. Scheele, D. et al. An oxytocin-induced facilitation of neural and emotional responses to social touch correlates inversely with autism traits. *Neuropsychopharmacology* **39**, 2078–2085 (2014).
24. de Waal, F. B. M. & Preston, S. D. Mammalian empathy: behavioural manifestations and neural basis. *Nat. Rev. Neurosci.* **18**, 498–509 (2017).
25. Silberberg, A. et al. Desire for social contact, not empathy, may explain "rescue" behavior in rats. *Anim. Cogn.* **17**, 609–618 (2014).
26. Bullmore, E. & Sporns, O. Complex brain networks: graph theoretical analysis of structural and functional systems. *Nat. Rev. Neurosci.* **10**, 186–198 (2009).
27. Staub, E. Helping a distressed person: social, personality, and stimulus determinants. *Adv. Exp. Soc. Psychol.*. **7**, 293–341 (1974).
28. Spear, L. P. Adolescent alcohol exposure: are there separable vulnerable periods within adolescence? *Physiol. Behav.* **148**, 122–130 (2015).
29. Brudzynski, S. M. Ethotransmission: communication of emotional states through ultrasonic vocalization in rats. *Curr. Opin. Neurobiol.* **23**, 310–317 (2013).
30. Marlin, B. J., Mitre, M., D'amour, J. A., Chao, M. V. & Froemke, R. C. Oxytocin enables maternal behaviour by balancing cortical inhibition. *Nature* **520**, 499–504 (2015).
31. Gimpl, G. & Fahrenholz, F. The oxytocin receptor system: structure, function, and regulation. *Physiol. Rev.* **81**, 629–683 (2001).
32. Power, J. D., Schlaggar, B. L., Lessov-Schlaggar, C. N. & Petersen, S. E. Evidence for hubs in human functional brain networks. *Neuron* **79**, 798–813 (2013).
33. Mikosz, M., Nowak, A., Werka, T. & Knapska, E. Sex differences in social modulation of learning in rats. *Sci. Rep.* **5**, 18114 (2015).
34. Choe, H. K. et al. Oxytocin mediates entrainment of sensory stimuli to social cues of opposing valence. *Neuron* **87**, 152–163 (2015).
35. Insel, T. R. & Fernald, R. D. How the brain processes social information: searching for the social brain. *Annu. Rev. Neurosci.* **27**, 697–722 (2004).
36. Valenta, J. G. & Rigby, M. K. Discrimination of the odor of stressed rats. *Science* **161**, 599–601 (1968).
37. Sotocinal, S. G. et al. The Rat Grimace Scale: a partially automated method for quantifying pain in the laboratory rat via facial expressions. *Mol. Pain.* **7**, 55 (2011).
38. Kiyokawa, Y. Social odors: alarm pheromones and social buffering. *Curr. Top. Behav. Neurosci.* **30**, 47–65 (2017).
39. Burgdorf, J. et al. Ultrasonic vocalizations of rats (*Rattus norvegicus*) during mating, play, and aggression: behavioral concomitants, relationship to reward, and self-administration of playback. *J. Comp. Psychol.* **122**, 357–367 (2008).
40. Oettl, L.L. & Kelsch, W. Oxytocin and olfaction. *Curr. Top. Behav. Neurosci.* (2017).
41. Langford, D. J. et al. Social approach to pain in laboratory mice. *Soc. Neurosci.* **5**, 163–170 (2010).
42. Ben-Ami Bartal, I., Rodgers, D. A., Bernardez Sarria, M. S., Decety, J. & Mason, P. Pro-social behavior in rats is modulated by social experience. *eLife* **3**, e01385 (2014).
43. de Waal, F. B. Putting the altruism back into altruism: the evolution of empathy. *Annu. Rev. Psychol.* **59**, 279–300 (2008).
44. Moaddab, M., Hyland, B. I. & Brown, C. H. Oxytocin excites nucleus accumbens shell neurons in vivo. *Mol. Cell. Neurosci.* **68**, 323–330 (2015).
45. Adolphs, R. The social brain: neural basis of social knowledge. *Annu. Rev. Psychol.* **60**, 693–716 (2009).
46. Bartz, J. A., Zaki, J., Bolger, N. & Ochsner, K. N. Social effects of oxytocin in humans: context and person matter. *Trends Cogn. Sci.* **15**, 301–309 (2011).
47. Decety, J. & Moriguchi, Y. The empathic brain and its dysfunction in psychiatric populations: implications for intervention across different clinical conditions. *Biopsychosoc. Med.*. **1**, 22 (2007).
48. Thioux, M. & Keysers, C. Empathy: shared circuits and their dysfunctions. *Dialog-. Clin. Neurosci.* **12**, 546–552 (2010).
49. LoParo, D. & Waldman, I. D. The oxytocin receptor gene (*OXTR*) is associated with autism spectrum disorder: a meta-analysis. *Mol. Psychiatry* **20**, 640–646 (2015).
50. Skuse, D. H. et al. Common polymorphism in the oxytocin receptor gene (*OXTR*) is associated with human social recognition skills. *Proc. Natl. Acad. Sci. USA* **111**, 1987–1992 (2014).
51. Paxinos, G. & Watson, C. *The Rat Brain Atlas in Stereotaxic Coordinates*. 4th edition, (Academic Press, San Diego, CA, USA, 1998).
55. Lukas, M., Toth, I., Veenema, A. H. & Neumann, I. D. Oxytocin mediates rodent social memory within the lateral septum and the medial amygdala depending on the relevance of the social stimulus: male juvenile versus female adult conspecifics. *Psychoneuroendocrinology* **38**, 916–926 (2013).

Acknowledgements

The authors thank M. Manning (University of Toledo) for providing OTRa, K. Deisseroth (Stanford University) for making optogenetic vectors freely available, and A. Veenema and D. Adams for discussions related to the project. Funding for this work was provided by the Boston College Undergraduate Research Fellowships; National Science Foundation Grant #1258923 to M.M.R.-C; NIH grants MH103401 to M.R. and MH093412 and MH109545 to J.P.C.; and Brain and Behavior Research Foundation grant No. 19417 to J.P.C.

Author contributions

Conceptualization: J.P.C., J.A.V., M.M.R.-C., M.R. Methodology: M.M.R.-C., J.A.V., M.R. J.P.C. Investigation: J.A.V., M.M.R.-C., K.B.G., A.P., M.M., M.R., J.P.C. Writing, original draft: J.A.V., M.M.R.-C., and J.P.C.;;revising & editing: M.M.R.-C., M.R., J.P.C. Funding acquisition, J.P.C., M.M.R.-C.

Competing interests

The authors declare no competing financial interests.

Additional information

Supplementary information accompanies this paper at https://doi.org/10.1038/s41593-018-0071-y.

Reprints and permissions information is available at www.nature.com/reprints.

Correspondence and requests for materials should be addressed to J.P.C.

Publisher's note: Springer Nature remains neutral with regard to jurisdictional claims in published maps and institutional affiliations.

Methods

Rats. Male and female Sprague-Dawley rats were obtained from Charles River Laboratories (Wilmington, MA). Rats were allowed a minimum of 7 d to acclimate to the vivarium after arrival and housed in groups of 2 or 3 with free access to food and water on a 12-h light/dark cycle. Behavioral procedures were conducted within the first 4 h of the light phase. All reagents and chemicals were purchased from Fisher Scientific, Tocris or Sigma unless otherwise noted. All procedures were conducted in accordance with the Public Health Service *Guide for the Care and Use of Laboratory Animals* and were approved by the Boston College Institutional Animal Care and Use Committee.

Social affective preference (SAP) test. The SAP test allowed quantification of social interactions initiated by an adult test rat when presented simultaneously with two unfamiliar conspecific stimuli. To begin the test, the adult test subject was placed into a clear plastic cage (50 × 40 × 20 cm, L × W × H) with a wire lid. Pairs of stimuli rats were either juvenile (PN 30 ± 2 d old) or adult (PN 50 ± 2 d old) and were placed inside one of two clear acrylic plastic enclosures (18 × 21 × 10 cm, L × W × H) on either end of the arena. Interaction between the experimental and stimuli rats was permitted on one side of the enclosure, which consisted of clear acrylic rods, spaced 1 cm center-to-center (see photo, Fig. 1) and as in ref. [52]. To habituate subjects to the procedure on days 1 and 2, the adult was placed in the arena for 60 min and then empty enclosures (day 1) or enclosures containing experimentally naive, unfamiliar stimuli rats (day 2) were added for 5 min. To assess social affective preference, on day 3 two unfamiliar stimuli rats were added, but one of the stimuli rats was exposed to two footshocks (1 mA, 5-s duration, 60-s intershock interval; Precision Regulated Animal Shocker, Coulbourn Instruments, Whitehall, PA) immediately before the 5-min test to induce a stressed affective state. Shock occurred in a separate room and shock parameters were selected because they were sufficient to produce a conditioned fear in our laboratory (data not shown). The 5-min test length was selected after pilot studies in which we observed a reliable decrease in social behavior after the first 5 min of test. In experiments involving optogenetics or intracerebral injections, a within-subjects design was employed such that each adult test subject was exposed to both vehicle and experimental treatments in SAP tests on consecutive days. A trained observer quantified the time spent in social interaction with each of the stimuli. Social interaction consisted of nose–nose and nose–body sniffing, and reaching into the enclosure to contact the stimulus rat. Digital video recordings were made of each test for later determination of inter-rater reliability by a second observer completely blind to the experimental manipulations and hypotheses. Across the experiments included in this report we observed very high inter-rater reliability, $r_{80} = 0.966$, $r^2 = 0.93$, $P < 0.0001$. Although conceived independently, this model has a number of features in common with the method recently reported with voles[21]. For some tests, we also quantified a number of behaviors in the experimental adult rat from videos, including time spent (i) sniffing or investigating the test arena, (ii) immobile, (iii) digging in the bedding, (iv) self-grooming and (v) biting or pulling at the conspecific. Videos were selected blind to SAP test social interaction results. The first three measures were assessed to quantify general locomotor activity, self-grooming has been argued to reflect emotion contagion[21] and biting may reflect aggressive behaviors.

One-on-one social exploration tests. As previously described[53], each experimental subject was placed into a plastic cage with shaved wood bedding and a wire lid 60 min before the test. To begin the test a juvenile or adult was introduced to the cage for 5 min, and exploratory behaviors (sniffing, pinning and allogrooming) initiated by the adult test subject were timed by an observer blind to treatment. Juvenile and adult stimuli rats were used for multiple tests but were never used more than once for the same adult test rat. Each experimental adult was given tests on consecutive days, once with an unfamiliar naive conspecific and once with an unfamiliar stressed conspecific (two footshocks, exactly as above); test order was counterbalanced.

Insular cortex cannula placement and microinjection. Under inhaled isoflurane anesthesia (2–5% v/v in O_2), cannula (26-gauge, Plastics One, Roanoke, VA) were inserted bilaterally into the insular cortex (from bregma: AP: −1.8 mm, ML: ±6.5 mm, DV: −6.2 mm from skull surface) and fixed in place with acrylic cement and stainless steel screws. Rat were administered the analgesic meloxicam (1 mg/kg, Eloxiject, Henry Schein) and antibiotic penicillin G (12,000 units, Combi-pen 48, Henry Schein) after surgery and allowed between 7 and 10 d recovery time before experimentation. The OTR antagonist (OTRa) desGly-NH_2-d$(CH_2)_5$[Tyr(Me)^2,Thr^{4}OVT[54], as in ref. [55], and OT were dissolved in sterile 0.9% saline vehicle, and the pan-PKC inhibitor Gö 6983 was first dissolved in 100% DMSO and then diluted to 200 nM in a vehicle of 10% DMSO and water. All injections were 0.5 µL per side and infused at a rate of 1 µL/min with an additional 1 min for diffusion. At the conclusion of the experiment, rats were overdosed with tribromoethanol (Sigma) and brains were dissected and sectioned at 40 µm to verify the microinjector tip location using cresyl violet stain and comparison to stereotaxic atlas[51]. Rats with occluded injectors or having cannula located outside of the insular cortex were excluded from all analyses (see Supplementary Fig. 6). To control for nonspecific effects of OTRa on social behavior, we conducted a control experiment in which OTRa had no effect on interaction between experimentally naive adult and PN 30 rats (Supplementary Fig. 10).

Optogenetics. Adult male rats underwent stereotaxic surgery to be implanted with bilateral guide cannula designed to fit a 200-µm optical fiber (Plastics One). After the cannula was secured, 250 nL of a viral vector containing the neuronal silencing halorhodopsin eNpHr3.0 under the CamKIIα promoter (AAV5-CamKIIα-eNpHR3.0-mCherry)[56] or a sham virus (AAV5-CamKIIα-YFP) was microinjected at a depth 1 mm below the termination of the guide cannula at a rate of 50 nL/min and allowed 5 min for diffusion. Optogenetic transductions were evaluated by fluorescence microscopy and in vitro whole cell recordings (Supplementary Fig. 5). During testing, a multimodal fiberoptic wire (200-µm core, 0.39 NA; Model FT200EMT, Thorlabs) extending 1 mm below the cannula tip was affixed to the stylet via a screw-top ferrule (Plastics One) and connected to a laser (GL523T3-100, Shanghai Laser & Optics Century). Throughout the length of a social test, green light (λ = 523 nm) at a power of ~10–15 mW/mm^2 was administered to maintain insular inhibition for the light ON conditions. During the light OFF condition, rats underwent the social test while connected to the laser but no light was administered. Functional photoinhibition was verified in whole-cell recordings of mCherry positive insular cortex pyramidal neurons in acute brain slices before, during and after green light administration (10 mW/mm2) delivered through the objective of the electrophysiology microscope. The extent of transfections was determined by imaging mCherry expression with widefield fluorescent microscopy (Zeiss AxioImager Z2). Locations of transfections are provided in Supplementary Figs. 5 and 6.

Electrophysiology solutions and drugs. All chemicals were purchased from Fisher Scientific, Sigma-Aldrich or Tocris. Standard artificial cerebrospinal fluid (aCSF) and recording solutions were used[57]. aCSF recording composition was (in mM) NaCl 125, KCl 2.5, $NaHCO_3$ 25, NaH_2PO_4 1.25, $MgCl_2$ 1, $CaCl_2$ 2 and glucose 10; pH = 7.40; 310 mOsm; aCSF cutting solution was: sucrose 75, NaCl 87, KCl 2.5, $NaHCO_3$ 25, NaH_2PO_4 1.25, $MgCl_2$ 7, $CaCl_2$ 0.5, glucose 25 and kynurenic acid 1; pH = 7.40, 312 mOsm. The internal recording solution consisted of (in mM) potassium gluconate 115, KCl 20, HEPES 10, Mg-ATP 2, Na-GTP 0.3 and sodium phosphocreatine 10; pH = 7.30; 278 mOsm with 0.1% biocytin. Kynurenic acid (1 mM) and SR-95531 (2 µM) were always added to the recording aCSF to block synaptic transmission for intrinsic recordings.

Insular cortex slices. Adult male rats were anesthetized with isoflurane, intracardially perfused with chilled (4 °C), oxygenated aCSF cutting solution and quickly decapitated. We took 300-µm coronal slices including the insular cortex using a vibratome (VT-1000S, Leica Microsystems, Nussloch, Germany). The slices were placed in oxygenated aCSF cutting solution (95% O^2 and 5% CO^2) at 37 °C for 30 min and then at room temperature (approximately 23 °C) for a minimum of 30 min before slices were used for electrophysiological recordings.

Electrophysiology. Whole-cell current-clamp recordings were obtained at 30 ± 2 °C. Patch-clamp electrodes were pulled (P-1000, Sutter Instruments, CA) from 1.5-mm outer diameter borosilicate glass (Sutter Instruments, CA) and filled with intracellular solution. Electrode resistance was 3–5 MΩ in the bath, and recordings were only included if the series resistance remained less than 30 MΩ with less than 10% change from baseline throughout the experiment. Slices were visualized using a 40× (0.75 NA) water-immersion objective under infrared differential interference contrast imaging on an upright microscope (AxioExaminer D1, Zeiss, Germany). All recordings were obtained with an Axon 700B amplifier and pClamp 10 (Molecular Devices), using appropriate bridge balance and electrode-capacitance compensation. After achieving a whole-cell configuration, baseline recordings were made in aCSF until 10 min of stable baseline were observed, at which point 500 nM oxytocin citrate was added to the bath. The dose of 500 nM was selected after a pilot study using a range of doses from 50 nM to 1 µM, the largest dose reported[58]. Because OT has high affinity for the vasopressin 1 A receptor (V1a), experiments typically isolate effects of OT to the OTR by using synthetic OTR agonists or a cocktail of OT and V1a antagonists. These steps were not taken here because, although V1a receptor mRNA has been reported throughout cortex[59], V1a receptor binding is not evident in adult male rat insula[60]. Analyses were performed using custom software written for Igor Pro (Wavemetrics Inc., Lake Oswego, OR).

As previously described[61], active properties were quantified from single spikes by holding the neuron at −67 mV, and 2.5-ms current pulses were injected to elicit a single AP. Passive properties were measured by holding the membrane potential at −67 mV and injecting 1-s current pulses through the patch electrode. The amplitudes of the current injections were between −300 pA and +400 pA in 50-pA steps. All traces in which APs were elicited were used to generate input–output curves as the total number of APs per second plotted against the injected current. EPSCs were made in the whole-cell configuration with the same internal solution and aCSF with tetrodotoxin (1 µM) added to some of the recordings (7 of 19 total cells) to isolate miniature EPSCs. However, in our recording conditions very few large events, (indicative of spontaneous glutamate release) occurred, so all events were assumed to be miniature EPSCs (mEPSCs) and the

data were pooled ($n = 19$). Recordings were made for 10 min before OT and then for 10 min after OT. mEPSC frequency and amplitude were determined with the mini analysis program (Synaptosoft). After recording, the slice was fixed in 4% paraformaldehyde and biocytin was visualized using the ABC method and NovaRed (Vector labs, Burlingame, CA). Only neurons with a pyramidal morphology and soma in deep layers of insular cortex were included for analysis. In a pilot experiment, no effect of OT was found on spontaneous inhibitory postsynaptic potentials (data not shown). The change in mEPSC amplitude observed likely reflects a postsynaptic modulation of AMPA receptor-mediated currents[62] but not an effect of OT on the spontaneous circuit activity per se. However, OT did not influence AMPA:NMDA current ratio (data not shown).

Evoked field excitatory postsynaptic potentials (fEPSPs) were recorded on a 6×10 perforated multiple electrode array (model: MCSMEA-S4-GR, Multichannel Systems) with integrated acquisition hardware (model: MCSUSB60) and analyzed with MC_Rack software (Version 3.9). Slices were placed on the array and adhered by suction of the perfusion through the perforated substrate. Bath solutions were as above and perfused through the slice from above. A stimulating electrode was selected in the deep layers of insular cortex, and fEPSPs were recorded after stimulation (0 to 5 V, biphasic 220 µs, 500-mV increments) before, during application of 500 nM OT, and after (wash). Each step in the I/O curve was repeated 3 times (20-s interstimulus interval) and each family of steps was replicated 3 times in each phase of the experiment. fEPSPs from channels displaying clear synaptic responses (as in Fig. 4b) and in the vicinity of the stimulating electrode were normalized to the individual channel's maximum response to 5-V stimulation at baseline; channels from the same slice were averaged for group analysis.

The electrophysiology experiments were replicated to test the dependence of OT effects on PKC. A few key aspects of the experiments were different. First, a between-groups design was used such that baseline measures were taken from all neurons after a stable recording was achieved. Then, drugs were bath-applied in aCSF that contained 0.5% DMSO to permit solubility of the pan-PKC inhibitor Gö 6983 (200 nM)[63]. The conditions were as follows: aCSF, aCSF with Gö 6983, OT (500 nM for whole cell recordings, 1 µM for fEPSPs), or OT with Gö 6983. The OT dose was increased to 1 µM in the fEPSP experiment as 500 nM did not reliably replicate the increase in fEPSPs when DMSO was added to the aCSF. All dependent measures were normalized to predrug baselines for analysis.

Ultrasonic vocalization recordings and analysis. Forty-four adult male rats were habituated for 1 h to the test arena and 24 h later randomly assigned to one of four treatment conditions: naive juvenile, naive adult, stressed juvenile or stressed adult in a 2×2 (stress×age) design ($n = 11$/group). Rats were given 5-min one-on-one social interaction tests as above with conspecifics according to their treatment group. To record USVs, an acrylic lid was placed over the arena with a 192-kHz USB microphone (Ultramic192K, http://www.dodotronic.com/) placed directly in the center. Recordings were made using Audacity 2.1 (http://www.audacityteam.org/), exported as.wav files, and audio spectrograms were generated in Raven Pro 1.5 (The Cornell Lab of Ornithology, https://store.birds.cornell.edu/Raven_Pro_p/ravenpro.htm). USVs were identified using the Band Limited Energy Detector function within Raven Pro. High frequency trill calls were found in the range of 8–20 ms, from 55–80 kHz; frequency-modulating rising calls were 30–100 ms, from 35–68 kHz; and 22-kHz flat calls were greater than 100 ms, from 18–28 kHz. These ranges were drawn from the literature[29], and detection parameters were refined for each recording based on visual inspection by a trained observer who was blind to treatment condition.

Fos analysis. After testing for USVs, each rat was left in the test cage alone and placed in a quiet room for 90 min, at which point the rat was overdosed with tribromoethanol and perfused with 0.01 M ice-cold, heparinized phosphate buffered saline (PBS) followed by 4% paraformaldehyde for later c-Fos analysis, as previously reported[52]. Brains were dissected and postfixed in 4% paraformaldehyde at 4 °C for 24 h and transferred to 30% sucrose for 2 d. We cut 40-µm coronal slices of the entire rostrocaudal extent of the brain via a cryostat at −19 °C and stored in 24-well plates containing cryoprotectant at 4 °C. To visualize c-Fos, floating sections quenched for endogenous peroxidase with 3% H_2O_2, blocked with 2% normal donkey serum in PBS-T (0.01% Triton-X 100), and then incubated overnight in rabbit anti-c-fos antibody (1:500, Cat. No. sc-52, Santa Cruz). Sections were then washed and incubated in biotinylated donkey anti-rabbit secondary antibody (1:200, Cat. No. 711-065-152, Jackson ImmunoResearch) using the avidin–biotin complex method (ABC Elite Kit, Cat. No. PK-6100, Vector Labs) with chromogen precipitate (NovaRed Kit, Cat. No. SK-4800, Vector Laboratories). Sections were floated onto glass slides, dehydrated, cleared and coverslipped with Permount. All steps were conducted at room temperature. To quantify c-Fos immunoreactive nuclei, tissue was imaged on a Zeiss Axioimager Z2 light microscope in the Boston College Imaging Core. Tiled images containing the ROIs were taken using a Zeiss AxioCam HRc digital camera through a 10× objective (N.A. 0.45). Representative images are provided in Supplementary Fig. 7. Using ImageJ software, images were converted to 16-bit, ROIs were traced with reference to the rat brain atlas and c-Fos immunoreactivity was quantified using the cell counter plug-in with parameters that were validated by comparison to manual counts by a trained observer. Cell density was computed the number of c-Fos immunoreactive cells divided by the ROI area (in pixels) for ANOVA and network analyses.

Statistical analysis. Sample sizes were initially determined based on prior work using social interaction[52,64] and intrinsic physiology[61]; no formal statistical methods were used to predetermine sample sizes. In all behavioral experiments, rats were randomly assigned to treatments. In electrophysiology experiments, cells were treated according to a Latin square design to achieve even representation of cells in treatment groups from different donor rats. For all of the experiments that entailed a mechanistic manipulation of the insular cortex including optogenetics, OT, OTRa and PKC inhibitor infusions, we observed a portion of rats that did not exhibit the expected behavior toward stress conspecifics. Therefore, rats were excluded from the statistical analysis if any of the following conditions were met: (i) they did not express the expected preference for stressed juveniles or avoidance of stressed adults was greater or less than 50% in the control condition, (ii) the cannula were occluded or found to be outside of the insula and/or (iii) virus expression was found to be unilateral or outside of the insula. The data from rats excluded due to item (i) above are provided for inspection in Supplementary Fig. 6. To compare differences between mean scores of social interaction and electrophysiological endpoints, we used *t* tests and analyses of variance (ANOVA). Individual replicate data are provided in the figures. In most experiments, there were within-subjects variables, which were treated as such in the analysis (paired-samples *t* test or repeated-measures ANOVA). The data distributions were visually inspected (all replicates are shown) and appeared to meet the assumptions for normality and equal variance, but these were not tested formally. Data were collected by observers blind to treatment. Final data analyses were not performed blind to the conditions of the experiments. Main effects and interactions were deemed significant when $P < 0.05$ and all reported post hoc test *P* values are Sidak-adjusted, to maintain an experiment-wise risk of type I errors at $\alpha = 0.05$. ANOVA were conducted in Prism 7.0c (GraphPad Software) and SPSS Statistics 24 (IBM).

Graph theoretical analysis has been applied to c-Fos datasets to characterize functional relationships in rodent neural circuits[65–68]. Network analyses were conducted with the Rubinov & Sporns (2010) Brain Connectivity Toolbox (https://sites.google.com/site/bctnet/) in Matlab R2015a (The Mathworks Inc.). We conducted a graph theoretical analysis on the c-Fos counts pooled across all treatment conditions to maximize network variation and to characterize the relationships among the ROIs, in which ROIs served as nodes and the rank-order correlations of c-Fos levels served as edges. Kendall's rank correlation was used to evaluate the relationships between each pair of the 29 included ROIs (nodes), computed across the sample of 44 rats that were used for USV analysis. Community detection analyses used a spectral community detection algorithm[69] applied to the weighted, unthresholded correlation network. Participation coefficients were calculated to determine the degree to which nodes participated in multiple networks, based on arguments that this measure is the most appropriate way to identify hubs in correlation-based networks[32]. Participation coefficients were based on positive edges only; additional network parameters are reported in Supplementary Fig. 8. Network visualization was conducted in R version 3.2.4 with the ggplot2[70] and ggnet (https://github.com/briatte/ggnet) packages.

Life Sciences Reporting Summary. Further information on experimental design is available in the Life Sciences Reporting Summary.

Code availability. Network analysis scripts are freely available at https://github.com/memobc. Igor scripts are available from the corresponding author upon reasonable request.

Data availability. The data that support the findings of this study are available from the corresponding author upon reasonable request.

References

52. Smith, C. J., Wilkins, K. B., Mogavero, J. N. & Veenema, A. H. Social novelty investigation in the juvenile rat: modulation by the µ-opioid system. *J. Neuroendocrinol.* **27**, 752–764 (2015).
53. Christianson, J. P. et al. Safety signals mitigate the consequences of uncontrollable stress via a circuit involving the sensory insular cortex and bed nucleus of the stria terminalis. *Biol. Psychiatry* **70**, 458–464 (2011).
54. Manning, M. et al. Oxytocin and vasopressin agonists and antagonists as research tools and potential therapeutics. *J. Neuroendocrinol.* **24**, 609–628 (2012).
56. Tye, K. M. et al. Amygdala circuitry mediating reversible and bidirectional control of anxiety. *Nature* **471**, 358–362 (2011).
57. Sidiropoulou, K. et al. Dopamine modulates an mGluR5-mediated depolarization underlying prefrontal persistent activity. *Nat. Neurosci.* **12**, 190–199 (2009).

58. Dölen, G., Darvishzadeh, A., Huang, K. W. & Malenka, R. C. Social reward requires coordinated activity of nucleus accumbens oxytocin and serotonin. *Nature* **501**, 179–184 (2013).
59. Szot, P., Bale, T. L. & Dorsa, D. M. Distribution of messenger RNA for the vasopressin V1a receptor in the CNS of male and female rats. *Brain Res. Mol. Brain Res.* **24**, 1–10 (1994).
60. Dumais, K. M. & Veenema, A. H. Vasopressin and oxytocin receptor systems in the brain: Sex differences and sex-specific regulation of social behavior. *Front. Neuroendocrinol.* **40**, 1–23 (2016).
61. Varela, J. A., Wang, J., Christianson, J. P., Maier, S. F. & Cooper, D. C. Control over stress, but not stress per se increases prefrontal cortical pyramidal neuron excitability. *J. Neurosci.* **32**, 12848–12853 (2012).
62. Turrigiano, G. G., Leslie, K. R., Desai, N. S., Rutherford, L. C. & Nelson, S. B. Activity-dependent scaling of quantal amplitude in neocortical neurons. *Nature* **391**, 892–896 (1998).
63. Gschwendt, M. et al. Inhibition of protein kinase C mu by various inhibitors. Differentiation from protein kinase c isoenzymes. *FEBS Lett.*. **392**, 77–80 (1996).
64. Christianson, J. P. et al. The sensory insular cortex mediates the stress-buffering effects of safety signals but not behavioral control. *J. Neurosci.* **28**, 13703–13711 (2008).
65. Vetere, G. et al. Chemogenetic interrogation of a brain-wide fear memory network in mice. *Neuron* **94**, 363–374.e4 (2017).
66. Wheeler, A. L. et al. Identification of a functional connectome for long-term fear memory in mice. *PLOS Comput. Biol.* **9**, e1002853 (2013).
67. Tanimizu, T. et al. Functional connectivity of multiple brain regions required for the consolidation of social recognition memory. *J. Neurosci.* **37**, 4103–4116 (2017).
68. Teles, M. C., Almeida, O., Lopes, J. S. & Oliveira, R. F. Social interactions elicit rapid shifts in functional connectivity in the social decision-making network of zebrafish. *Proc. Biol. Sci.*. **282**, 20151099 (2015).
69. Newman, M. E. Modularity and community structure in networks. *Proc. Natl. Acad. Sci. USA* **103**, 8577–8582 (2006).
70. Wickham, H. *ggplot2: Elegant Graphics for Data Analysis*. (Springer-Verlag, New York, 2009).

nature neuroscience

SUPPLEMENTARY INFORMATION

https://doi.org/10.1038/s41593-018-0071-y

In the format provided by the authors and unedited.

Insular cortex mediates approach and avoidance responses to social affective stimuli

Morgan M. Rogers-Carter, Juan A. Varela, Katherine B. Gribbons, Anne F. Pierce, Morgan T. McGoey, Maureen Ritchey and John P. Christianson*

Department of Psychology, Boston College, Chestnut Hill, MA, USA. Morgan M. Rogers-Carter and Juan A. Varela contributed equally to this work.
*e-mail: j.christianson@bc.edu

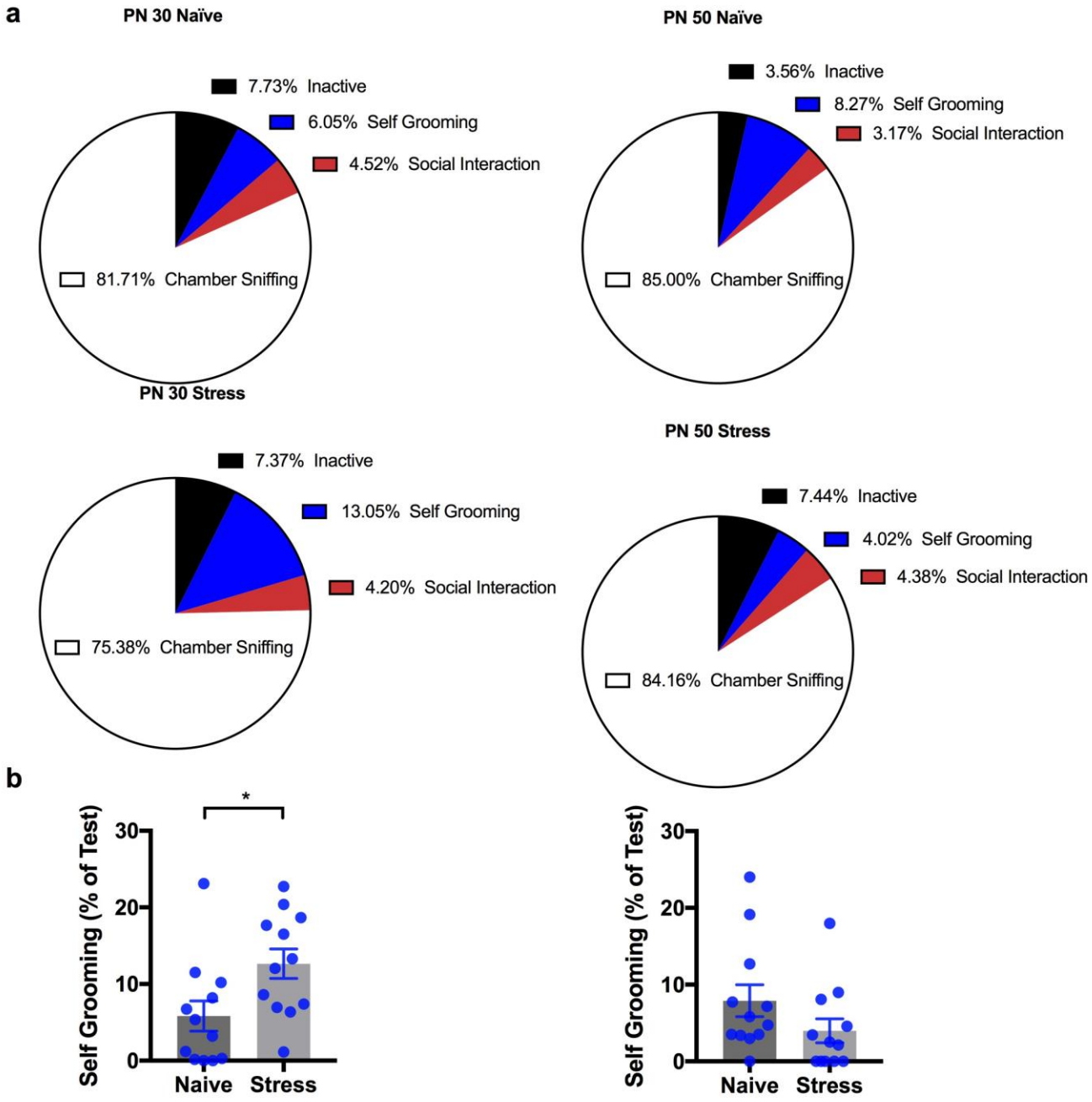

Supplementary Figure 1

Conspecific behavior in social affective preference test.
(a) An observer blind to conspecific treatment tallied the time spent inactive, self-grooming, engaged in social interaction with the experimental adult and time spent sniffing and exploring the conspecific chamber of 12 pairs of target rats from each of the PN 30 and PN 50 treatment groups. The average portion (% of total) time spent in each behavior during the 5-minute test is shown for each treatment. The analyses indicate that the conspecifics spent the majority of time in active behaviors, namely sniffing and exploring the chamber. **(b)** Mean (+/- SEM) time spent self-grooming. Separate t-tests were conducted to compare time in each behavior and revealed a significant increase in self grooming after stress in the PN 30 group. *$t(22) = 2.47$, $p = 0.022$ (2-tailed). No other comparisons reached significance, and self grooming did not correlate with behavior of the experimental adult rats.

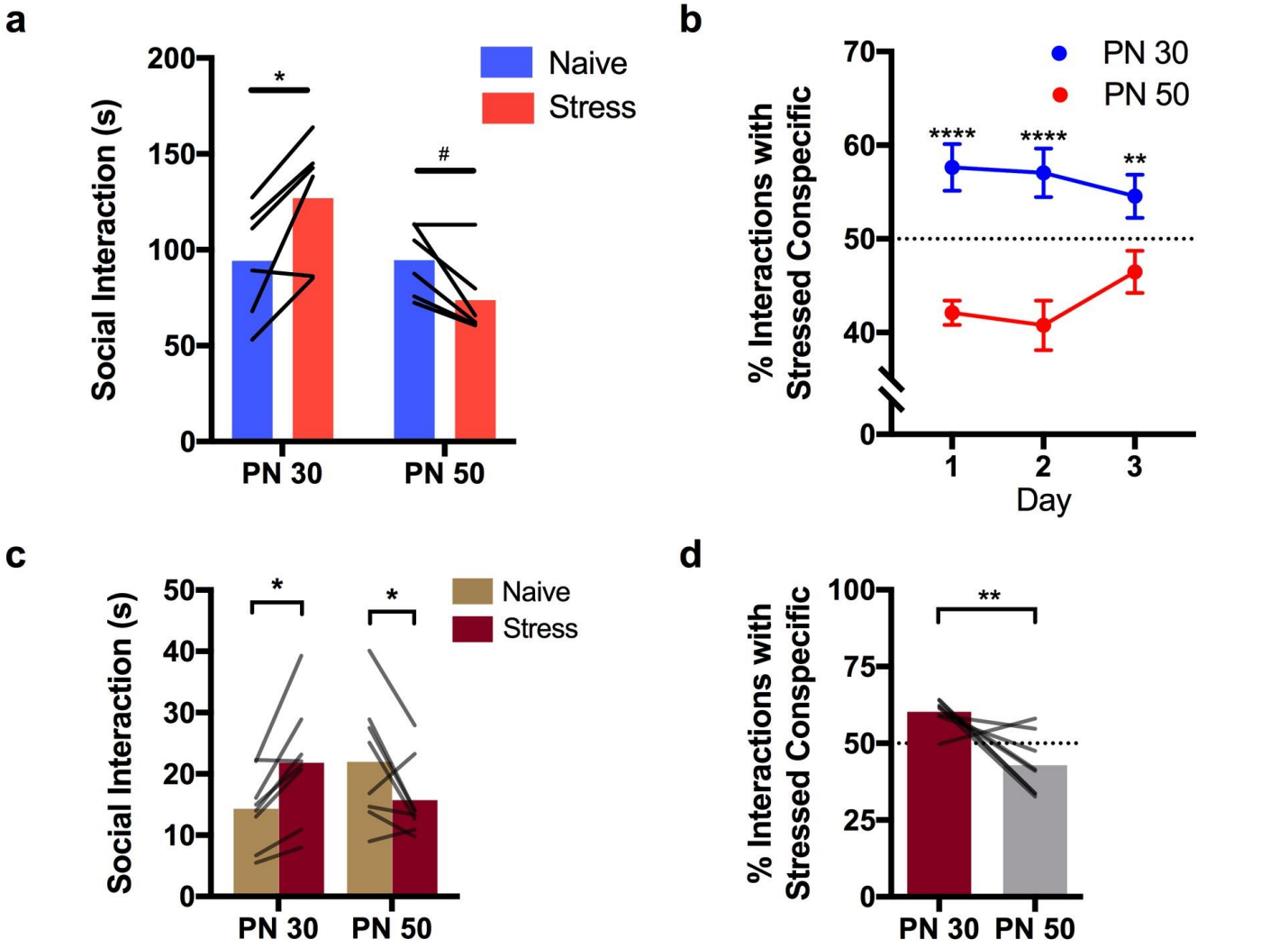

Supplementary Figure 2

Repeated one-on-one testing and SAP tests in females.
(a) Adult male rats (n = 6) were given a series of 4, 1-on-1 social interaction tests (5 min duration) in each of the following conditions: naive-juvenile, naive-adult, stress-juvenile and stress-adult; test order was counter balanced using a Latin square design. Tests were exactly as described in the Online Methods and separated by 20 to 30 min. All conspecific stimuli were novel/unfamiliar pairs. Two way repeated measures ANOVA revealed significant interaction of age and stress, $F(1, 5) = 20.549$, $p = 0.006$, with significant differences between Naive and Stress at both ages, *p = 0.022 (2-tailed), #p = 0.028 (1-tailed). **(b)** Mean (+/- SEM, n = 6) percent preference for stressed conspecific. This series of tests in (a) was repeated for 3 consecutive days and data were converted to percent preference for the stressed conspecific by age, and by day. PN30 and PN50 preference scores were significantly different on all three days. ANOVA revealed significant Age & Day interaction $F(2, 10) = 5.211$, $p = 0.028$, ****p<0.0001, **p<0.007 (Sidak). **(c)** Mean social interaction time. SAP tests were performed on adult female, regularly cycling rats with pairs of male juvenile or adult conspecifics as interaction stimuli (N=8 females). SAP tests were exactly as described in the online methods. A significant 2-way interaction, $F(1, 14) = 15.52$, $p = 0.002$ indicated that the females also exhibit preference to interact with stressed juvenile conspecifics but avoid stressed adults, *p<0.05 (Sidak). **(d)** Results in c. shown as Mean % time interacting with stressed conspecific for comparison, **$t(7) = 3.51$, $p = 0.009$ (2-tailed).

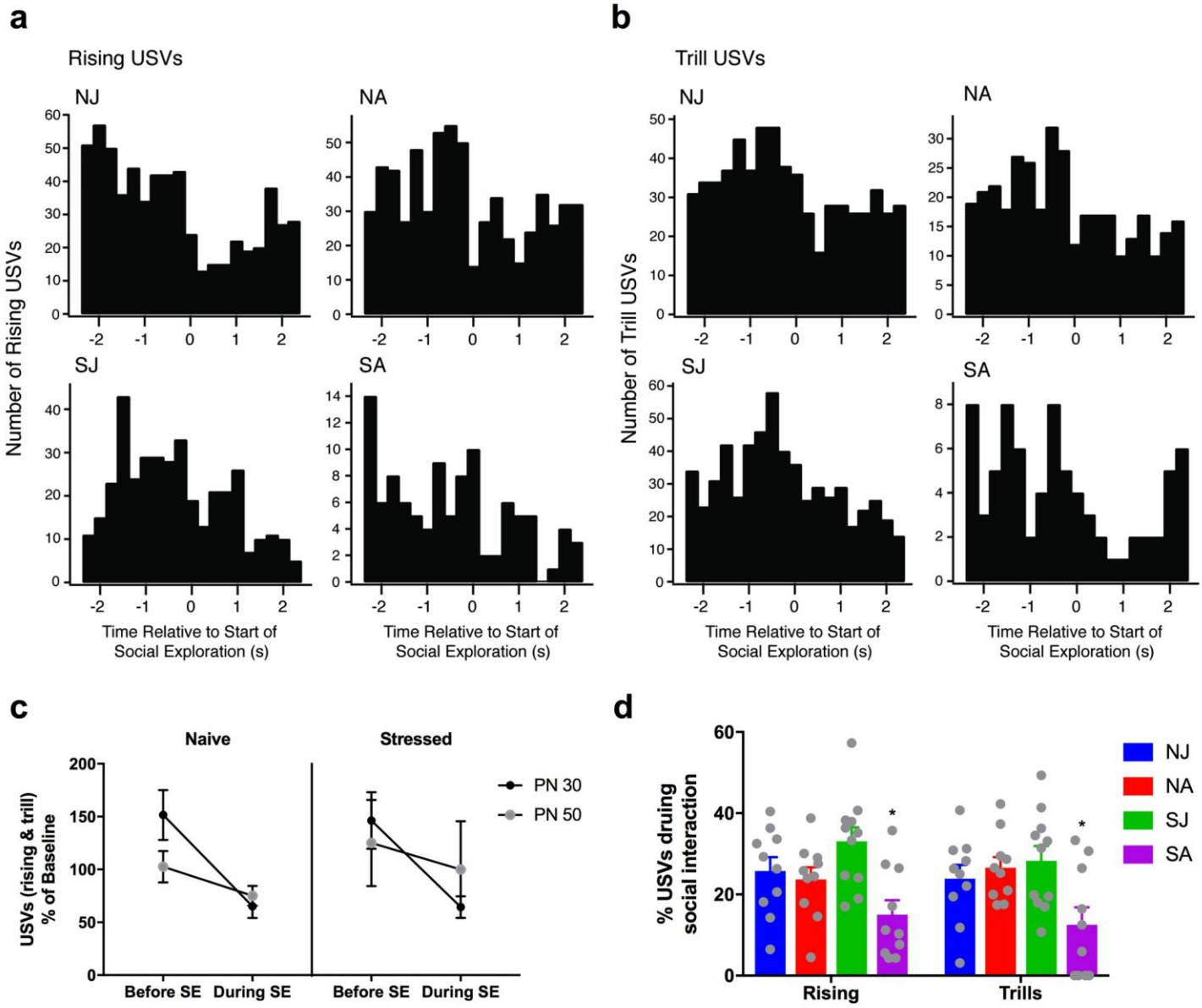

Supplementary Figure 3

Ultrasonic vocalizations and social interaction.
Extended analysis of data described in Figure 1I-K. Peri-event histograms showing frequency of Rising **(A)** and Trill **(B)** USVs in the different conspecific treatment conditions (NJ, n = 10, NA, n = 10, SJ, n = 11, SA, n = 11). Time 0 is equal to the beginning of a social interaction bout. Bins are 250ms. Calls were included from all rats in the treatment condition for social interaction bouts 3s or longer. **(C)** Mean (+/- S.E.M.) rate of vocalization (rising and trills combined) 2.5 s before and 2.5 s after the beginning of a 3 s (or longer) social interaction bout. Values normalized to a pre-bout baseline 5 s prior to the social interaction. **(D)** Mean (+ S.E.M.) percent of total USVs detected during 5 minute social interaction bout that occurred during social interactions. Stress reduced within-bout vocalizations in the adult condition (Main effect of Age, $F(3, 74) = 8.523$, $p < 0.0001$). *SA vs. NJ, $p = 0.019$; SA vs. NA, $p = 0.016$; SA vs. SJ, $p = 0.0005$ (Fisher LSD). NJ = naive juvenile, NA = naive adult, SJ = stressed juvenile, SA = stressed adult.

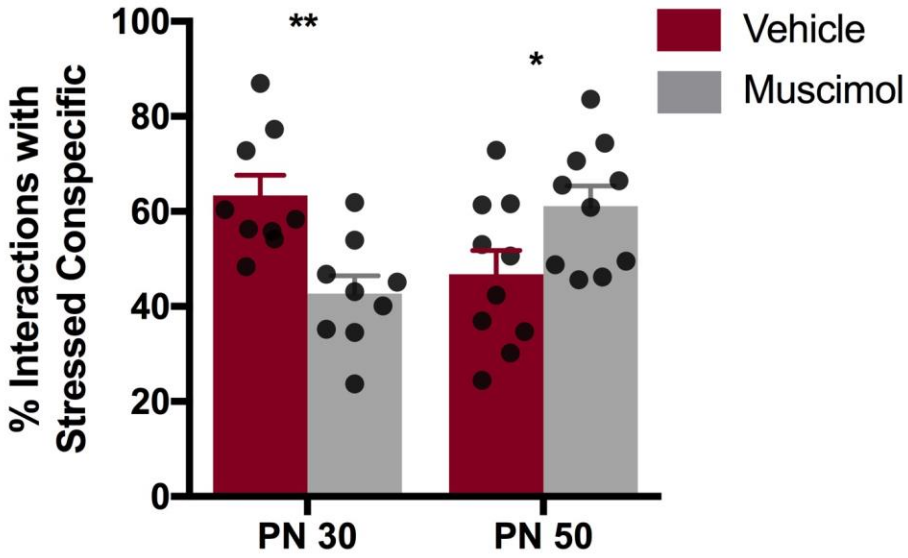

Supplementary Figure 4

Inhibition of insular cortex with muscimol reverses SAP test behavior.
In a pilot study, rats were implanted with insular cortex cannula for microinjection exactly as described in the online methods. After 7 days of recovery rats received SAP tests with either PN 30 (n = 9) or PN 50 (n = 10) conspecifics. SAP tests were as in Figure 2: Habituation to arena on Day 1, Habituation with exposure to naïve conspecifics on Day 2, and SAP tests with one conspecific exposed to 2 footshocks prior to test on Day 3. Either Vehicle (0.9% saline) or muscimol (100ng/side in saline) was injected to the insular cortex 60 minutes prior to SAP tests on day 3. This experiment was different in design from the others included in the main text because rats received only 1 SAP test precluding the more powerful within-subject comparisons of drug effect. SAP behavior is shown as the mean (+/- SEM) percent of time spent interacting with the stressed conspecific of the total time spent in social interaction during the SAP test. A 2-way between subjects ANOVA revealed a significant Age by Drug interaction, $F(1, 34) = 16.27$, $p < 0.001$. Post hoc comparisons between drug conditions within each age revealed a significant decrease in time spent interacting with the stressed PN 30 juvenile conspecific by muscimol (**$p = 0.005$, Sidak) and a significant increase in time spent interacting with the stressed PN 50 adult conspecific (*$p = 0.043$, Sidak).

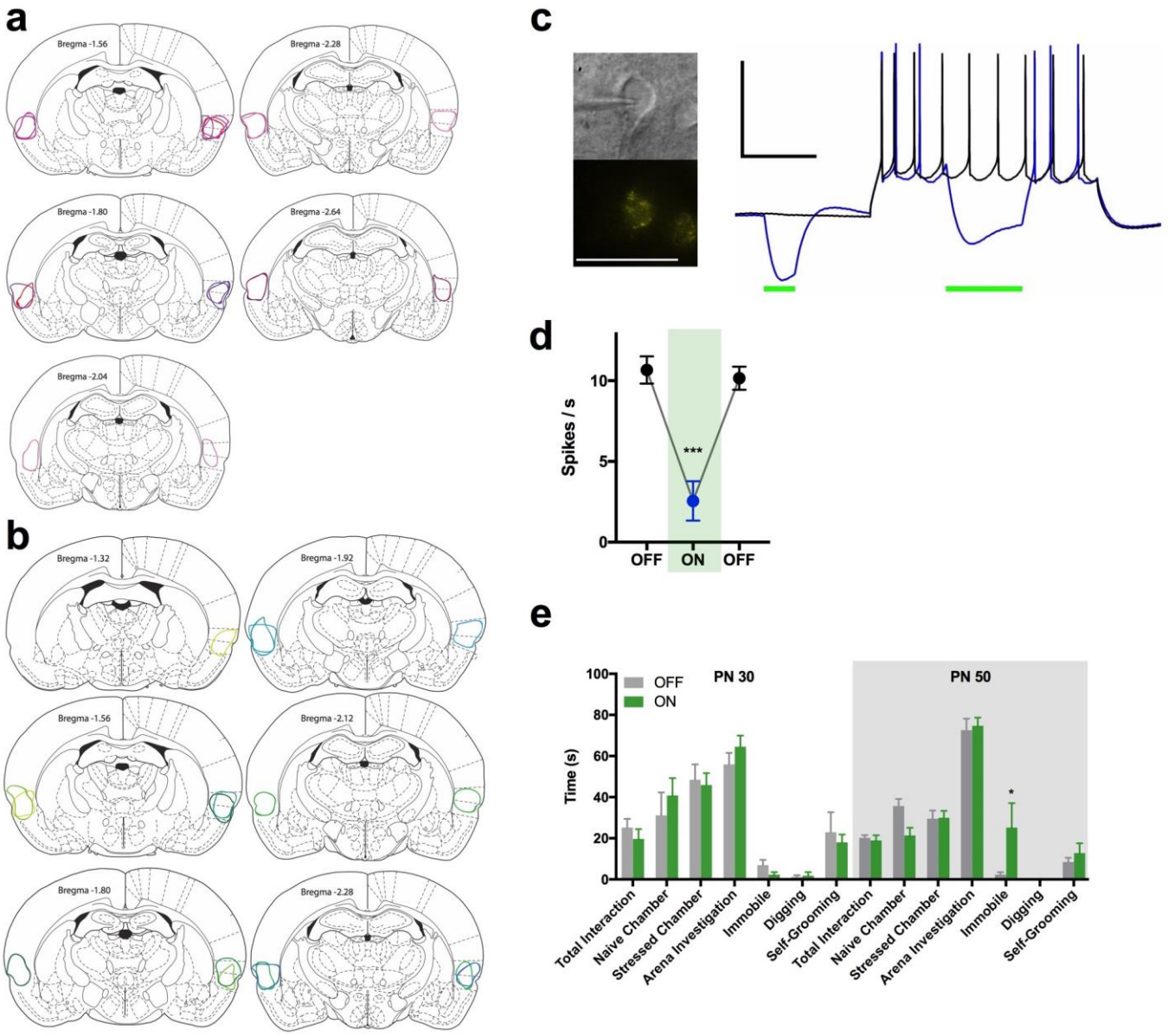

Supplementary Figure 5

Verification of halorhodopsin transductions and behavioral analysis in SAP tests.

Placement of AAV5-CamKIIa-eNpHr3.0-mCherry transfections in experimental adult rats given SAP tests with **(a)** PN 30 juvenile conspecifics or **(b)** PN 50 conspecifics. Different colored traces correspond to individual replicates. In each case the tip of the fiber optic cannula was found within the insular cortex and either directly above or within the area marked as containing mCherry (unamplified) fluorescence. **(c)** Viral transfer was validated in whole cell recordings of mCherry (above DIC image, below mCherry false colored yellow. 40x, Scale bar = 40μm) positive neurons in acute slices containing the insular cortex. Application of green light (wavelength = 532nm, 10mW/mm^2) through the objective of the electrophysiology microscope induced robust hyperpolarizations which silenced spiking when provided during a train of evoked spikes, scale bar 50mV/250ms. **(d)** Mean (+/- SEM) spikes during sequence of OFF/ON/OFF application as in panel (D), n = 6 cells, one-way repeated measures ANOVA, $F(2, 15) = 22.82$, $p < 0.0001$ with the spike rate in the ON condition significantly less than either off condition, ***$p < 0.0001$ (Sidak). **(e)** Mean (+SEM) time spent in different behaviors of adult conspecifics in optogenetic experiment (PN30, n=9, PN50, n=11). Behavior levels are equal between light ON and OFF conditions except for increased immobility in the PN50 light ON condition, Age by Light by Behavior interaction, $F(4, 60) = 3.01$, $p = 0.025$. *$p = 0.001$ (Sidak). The increase in immobility is likely due to 2 of 11 rats that exhibited very high immobility (25-26s). Brain Atlas illustrations were reproduced with permission as previously published in *The Brain Atlas in Stereotaxic Coordinates*, 4th Edition, Paxinos, G. & Watson, C. Pages 296, 303, 306-317 & 332. Copyright Elsevier (1998).

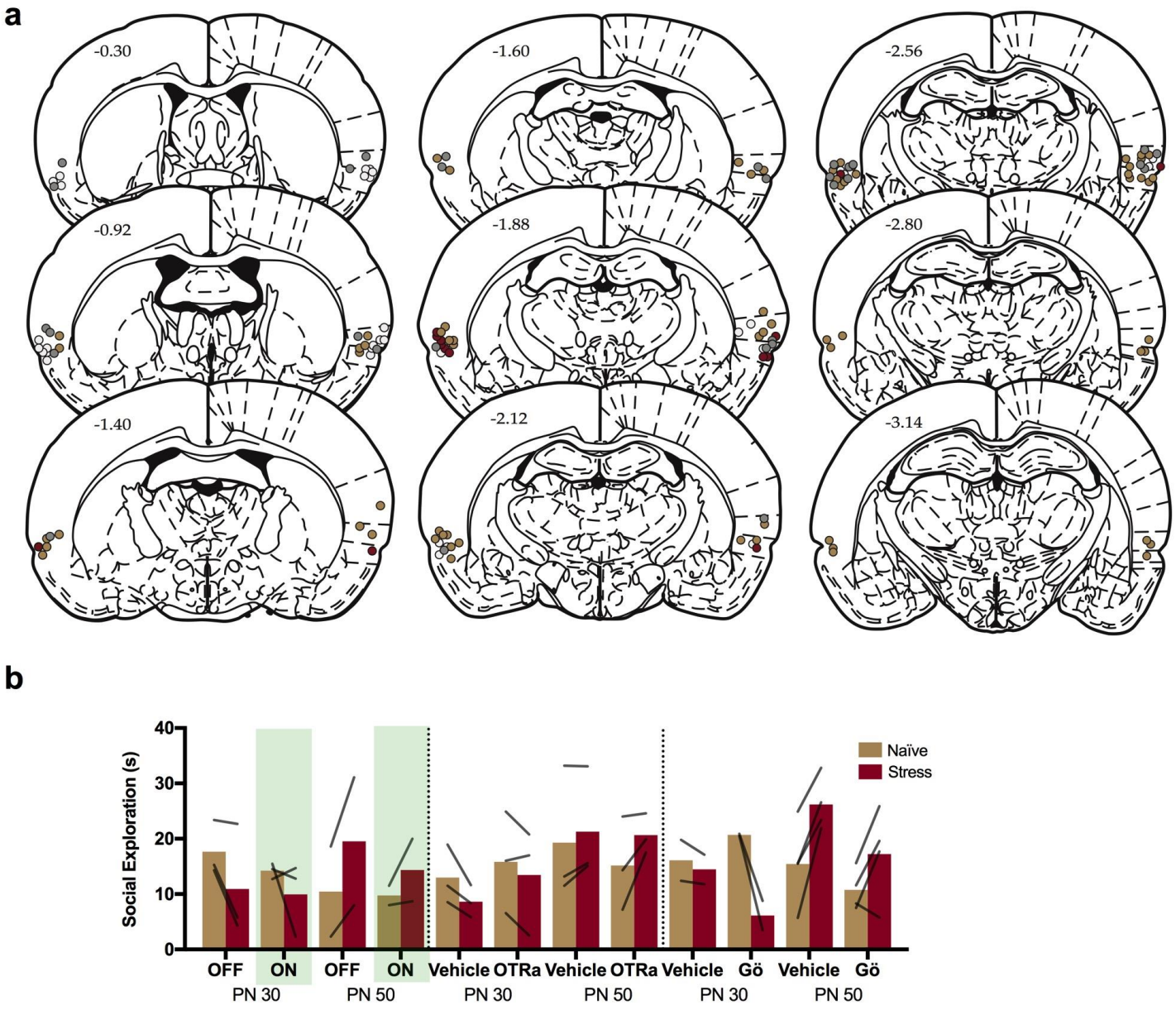

Supplementary Figure 6

Placement of cannula tips for microinjection experiments and excluded subject data.
(a) Cannula tip placement within the insular cortex was verified in 40μm fresh frozen sections stained with Cresyl Violet under light microscopy. Tip locations are indicated. Section distance from Bregma indicated in mm. Open/White Circles relate to Figure 5B-C, Red circles relate to Figure 5E and Gold circles to Figure 5F, Grey circles related to Figure 5G-H. **(b)** SAP test behavior from the rats excluded from mechanistic experiments because the baseline behavior (light OFF or vehicle condition) did not reflect the phenomena under study. LEFT: excluded from Figure 2F-G, CENTER: excluded from Figure 5B-C, RIGHT: excluded from Figure 5G-H. Brain Atlas illustrations were reproduced with permission as previously published in *The Brain Atlas in Stereotaxic Coordinates*, 4th Edition, Paxinos, G. & Watson, C. Pages 296, 303, 306-317 & 332. Copyright Elsevier (1998).

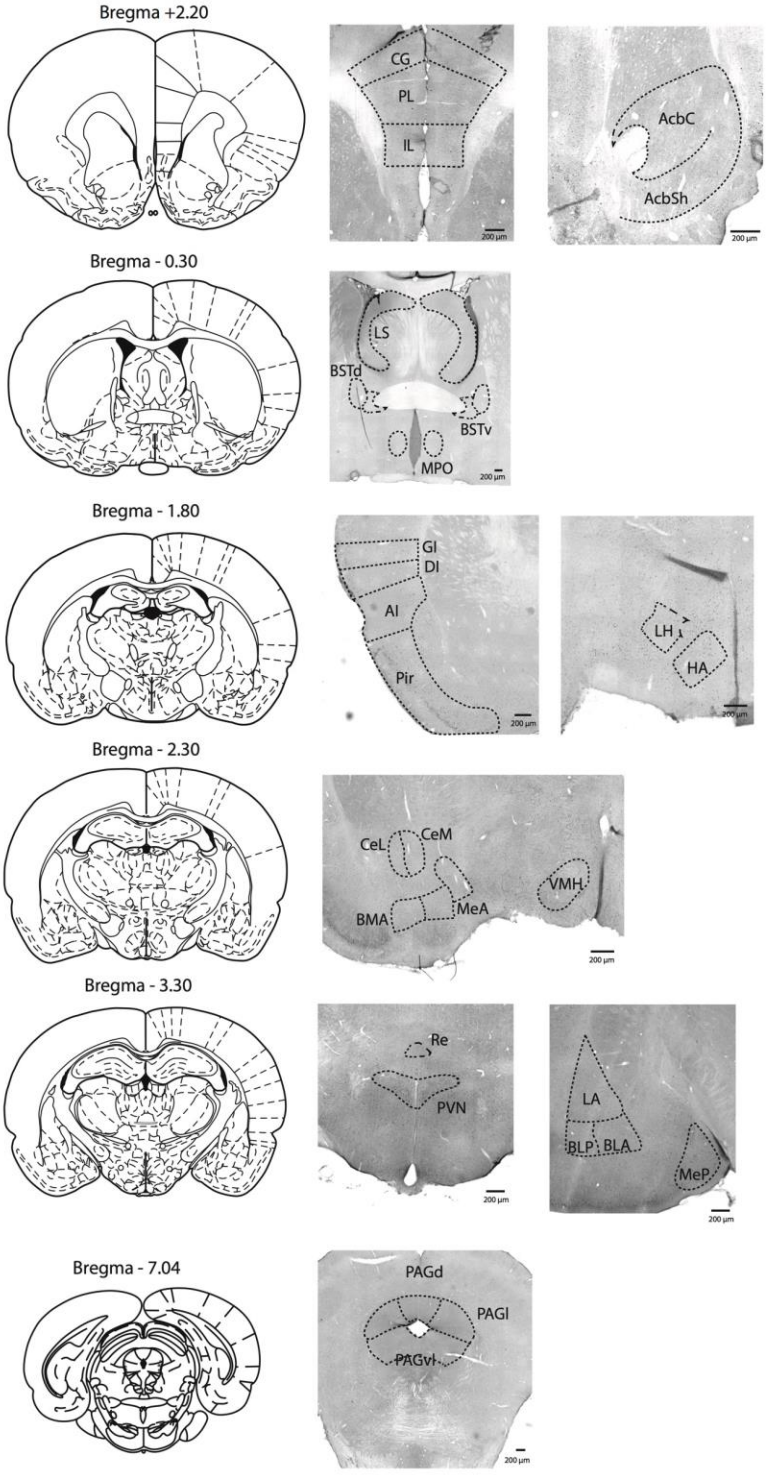

Supplementary Figure 7

Representative examples of c-Fos immunohistochemistry and regions of interest.
Coronal diagrams on left correspond to regions of interest indicated within the representative digital photomicrographs on the right. Images were acquired and analyzed with equal exposure and analysis was conducted on images without adjustments to brightness or contrast. The representative images have been adjusted to facilitate presentation. This experiment was replicated 11 times per group. List of abbreviations is provided in Supplementary Figure 8. Scale bars = 200μm. Brain Atlas illustrations were reproduced with permission as previously published in *The Brain Atlas in Stereotaxic Coordinates*, 4th Edition, Paxinos, G. & Watson, C. Pages 296, 303, 306-317 & 332. Copyright Elsevier (1998).

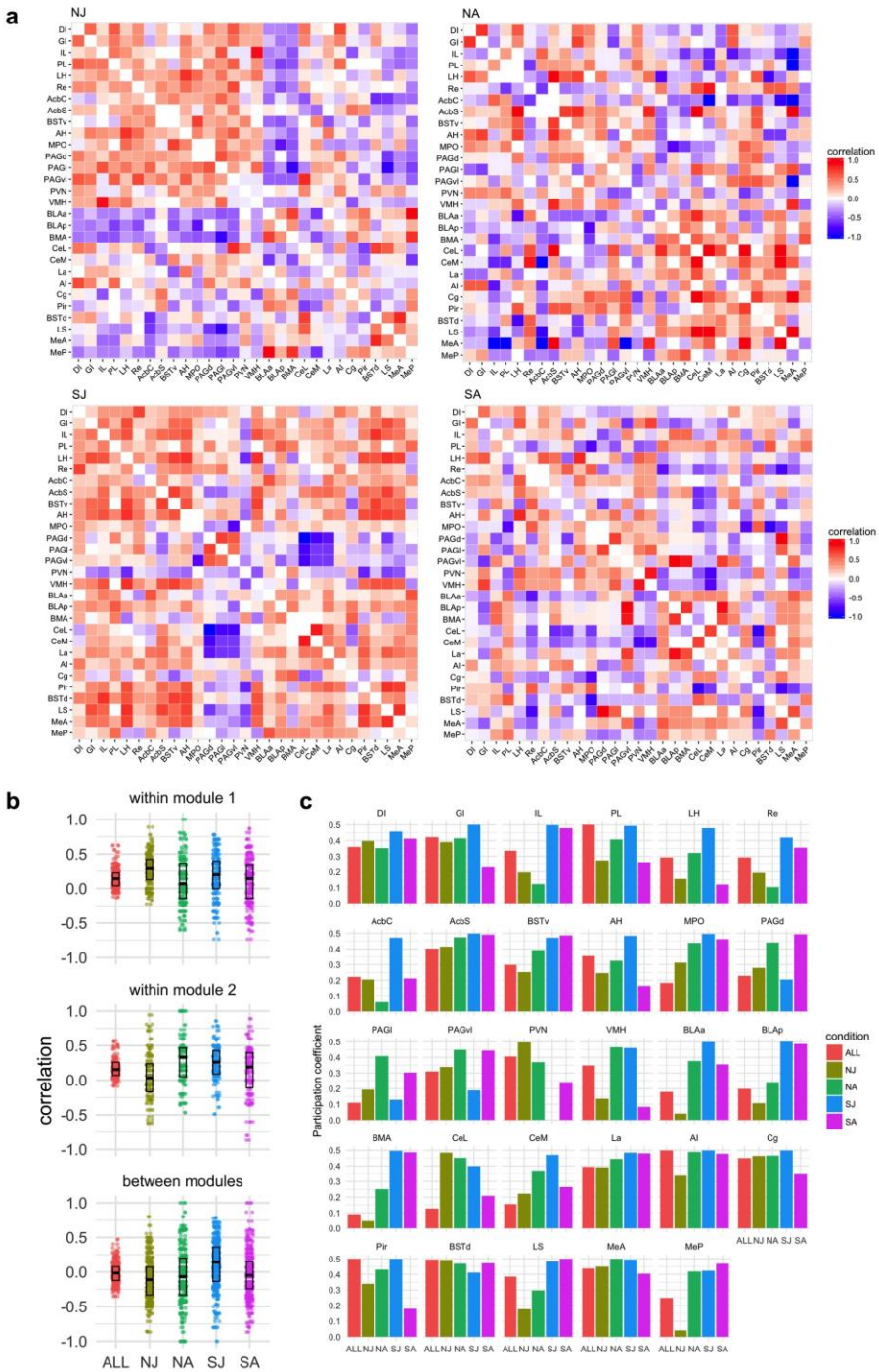

Supplementary Figure 8

Extended analysis of Fos network.

(A) Correlation matrices (Kendall's tau) organized as in Fig. 6 by conspecific age and stress condition (n=11/group, N=44 for All condition). **(B)** Correlations (Box plots range = 25th to 75th percentile, line indicates median) within and between modules identified by a community detection analysis (described in Fig. 6B). **(C)** Effect of stress on participation coefficient computed as in Fig. 6 (ALL condition) and for each age and stress condition. NJ = naive juvenile, NA = naive adult, SJ = stressed juvenile, SA = stressed adult. See Sup. Table 1 for abbreviation key.

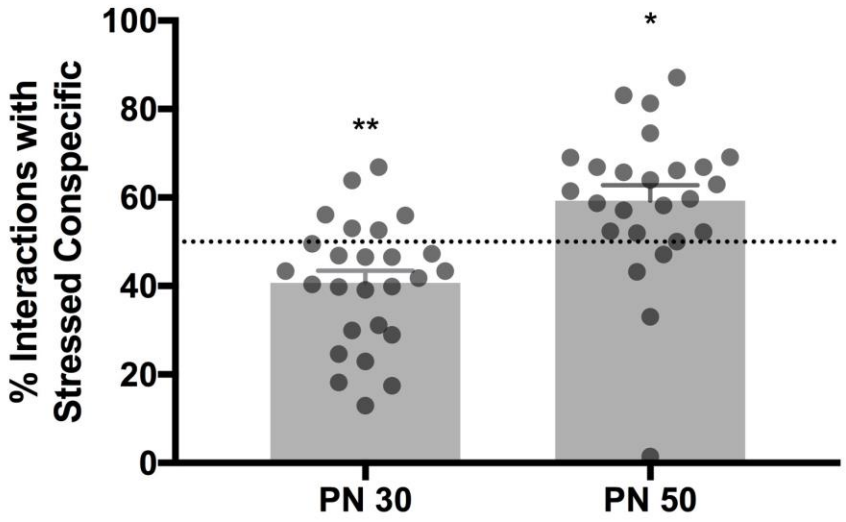

Supplementary Figure 9

Manipulations of insular cortex reverse SAP test behavior.

From visual inspection of the results of the optogenetic and pharmacology experiments it appeared that manipulating the insular cortex not only prevented the expression of preference behavior in the SAP test, but that it might actually switch preference in the opposite direction. To test this possibility, % time interacting with the stressed conspecific scores were pooled from all of the mechanistic experiments (halorhodopsin, OTRa, PKC inhibitor, n = 26 for PN30, n=25 for PN50) and we conducted one-sample t-tests (2-tailed) comparing each condition to 50% (no preference). Indeed, disrupting insular function reversed SAP behavior. In PN30 rats, the mean (+SEM) % time interacting with the stressed conspecific switched away from the stressed juvenile, $t(25) = 3.35$, $^{**}p = 0.003$ and in PN 50 rats it switched toward interacting with the stressed adult, $t(24) = 2.30$, $^{*}p = 0.013$.

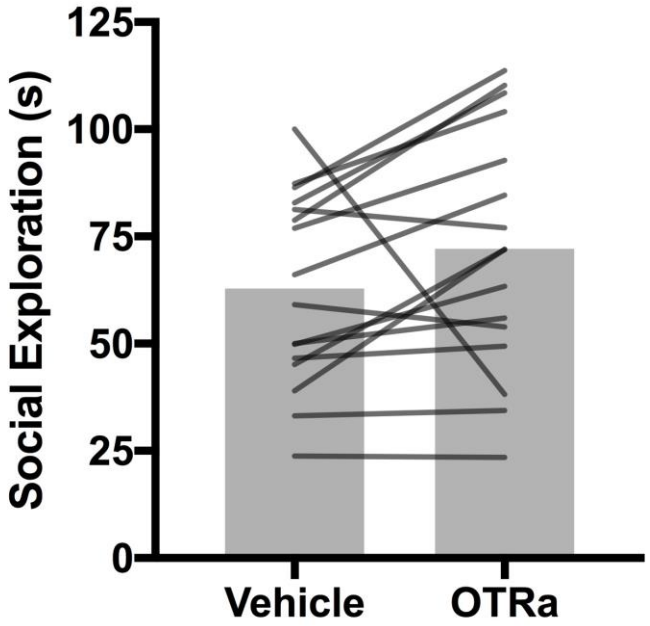

Supplementary Figure 10

Intra-insula oxytocin receptor antagonist (OTRa) does not alter social interaction.

Adult male rats were implanted with insular cortex cannula and given 3 minute social interaction tests with naive, juvenile conspecifics (N=16). Vehicle or OTRa (as described in Online Methods) was injected 15 min before testing on day 1 or day 2. All rats were tested under both drug conditions with test order counterbalanced. There was no effect of OTRa on social interaction $t(15) = 1.61$, $p = 0.13$ (2-tailed).

nature research

Corresponding author(s): John Christianson

Life Sciences Reporting Summary

Nature Research wishes to improve the reproducibility of the work that we publish. This form is intended for publication with all accepted life science papers and provides structure for consistency and transparency in reporting. Every life science submission will use this form; some list items might not apply to an individual manuscript, but all fields must be completed for clarity.

For further information on the points included in this form, see Reporting Life Sciences Research. For further information on Nature Research policies, including our data availability policy, see Authors & Referees and the Editorial Policy Checklist.

Please do not complete any field with "not applicable" or n/a. Refer to the help text for what text to use if an item is not relevant to your study.
For final submission: please carefully check your responses for accuracy; you will not be able to make changes later.

Experimental design

1. Sample size

   Describe how sample size was determined.

   Samples were selected based on prior work in social behavior and electrophysiology. This is stated on page 38 in the sub section "Statistical Analysis."

2. Data exclusions

   Describe any data exclusions.

   Behavioral data were excluded when cannula placements or transductions were found outside of the insular cortex, when rats in the vehicle or light OFF conditions did not exhibit preference for the stressed juvenile, or avoidance of the stressed adult. These data were analyzed separately and are presented in Sup. Fig. S6. Regarding ephys data, data were excluded if 1) series resistance exceeded 30Mohm or changed more than 10% from baseline, 2) if the neuron was found outside of the insular region of interest or 3) the neuron was found to have non-pyramidal morphology.

3. Replication

   Describe the measures taken to verify the reproducibility of the experimental findings.

   The key phenomena are replicated several times within this manuscript. We have several additional replications in complementary experiments (not included in the manuscript).

4. Randomization

   Describe how samples/organisms/participants were allocated into experimental groups.

   Rats/neurons were randomly assigned to treatments, and to order of treatment at the outset of each experiment. Counterbalancing was used to control for order effects.

5. Blinding

   Describe whether the investigators were blinded to group allocation during data collection and/or analysis.

   Behavioral studies in which complete blinding was impossible during live scoring of behavior, a treatment blind observer also scored the tests from video and inter-rater-reliability is reported in the Online Methods.

Note: all in vivo studies must report how sample size was determined and whether blinding and randomization were used.

6. Statistical parameters

For all figures and tables that use statistical methods, confirm that the following items are present in relevant figure legends (or in the Methods section if additional space is needed).

n/a	Confirmed
☐	☒ The exact sample size (*n*) for each experimental group/condition, given as a discrete number and unit of measurement (animals, litters, cultures, etc.)
☐	☒ A description of how samples were collected, noting whether measurements were taken from distinct samples or whether the same sample was measured repeatedly
☐	☒ A statement indicating how many times each experiment was replicated
☐	☒ The statistical test(s) used and whether they are one- or two-sided *Only common tests should be described solely by name; describe more complex techniques in the Methods section.*
☐	☒ A description of any assumptions or corrections, such as an adjustment for multiple comparisons
☐	☒ Test values indicating whether an effect is present *Provide confidence intervals or give results of significance tests (e.g. P values) as exact values whenever appropriate and with effect sizes noted.*
☐	☒ A clear description of statistics including central tendency (e.g. median, mean) and variation (e.g. standard deviation, interquartile range)
☐	☒ Clearly defined error bars in all relevant figure captions (with explicit mention of central tendency and variation)

See the web collection on statistics for biologists for further resources and guidance.

Software

Policy information about availability of computer code

7. Software

Describe the software used to analyze the data in this study.	Igor Pro, MC_Rack v.3.9, Image J and cell counter plug-in, GraphPad Prism 7, SPSS statistics 24, MATLab R5015a with Rubinov and Sporn's Brain Connectivity Toolbox, Synaptosof Mini Analysis Program v. 6.0.7, RavenPro 1.5, Audacity 2.1, R v 3.2.4. Custom R scripts are available at https://github.com/memobc.

For manuscripts utilizing custom algorithms or software that are central to the paper but not yet described in the published literature, software must be made available to editors and reviewers upon request. We strongly encourage code deposition in a community repository (e.g. GitHub). *Nature Methods* guidance for providing algorithms and software for publication provides further information on this topic.

Materials and reagents

Policy information about availability of materials

8. Materials availability

Indicate whether there are restrictions on availability of unique materials or if these materials are only available for distribution by a third party.	There are no restrictions

9. Antibodies

Describe the antibodies used and how they were validated for use in the system under study (i.e. assay and species).	Sc-52 Rabbit-anti cFos was used (Santa Cruz) which has been widely validated for detection of Fos in rat. These are described in the Online Methods section.

10. Eukaryotic cell lines

a. State the source of each eukaryotic cell line used.	no eukaryotic cell lines were used
b. Describe the method of cell line authentication used.	*Describe the authentication procedures for each cell line used OR declare that none of the cell lines used have been authenticated OR state that no eukaryotic cell lines were used.*
c. Report whether the cell lines were tested for mycoplasma contamination.	*Confirm that all cell lines tested negative for mycoplasma contamination OR describe the results of the testing for mycoplasma contamination OR declare that the cell lines were not tested for mycoplasma contamination OR state that no eukaryotic cell lines were used.*
d. If any of the cell lines used are listed in the database of commonly misidentified cell lines maintained by ICLAC, provide a scientific rationale for their use.	*Provide a rationale for the use of commonly misidentified cell lines OR state that no commonly misidentified cell lines were used.*

Animals and human research participants

Policy information about studies involving animals; when reporting animal research, follow the ARRIVE guidelines

11. Description of research animals

Provide all relevant details on animals and/or animal-derived materials used in the study.

Sprague-Dawley (CD Derived) male rats were used in all experiments (except Female adults (60-80 days old were used in Sup. Fig. 2) and were obtained form Charles River Laboratories. Experimental Adult rats were 60-80 days old at the time of testing (behavioral and ephys experiments). Conspecifics were 30(+/- 2) or 50(+/-2) days old at the time of testing.

Policy information about studies involving human research participants

12. Description of human research participants

Describe the covariate-relevant population characteristics of the human research participants.

This study did not use human participants.